

See discussions, stats, and author profiles for this publication at: <https://www.researchgate.net/publication/233907899>

# Synthesis and Characterization of DNA Minor Groove Binding Alkylating Agents

ARTICLE *in* CHEMICAL RESEARCH IN TOXICOLOGY · DECEMBER 2012

Impact Factor: 3.53 · DOI: 10.1021/tx300437x · Source: PubMed

---

CITATIONS

7

READS

72

## 12 AUTHORS, INCLUDING:



Ajay Srinivasan

10 PUBLICATIONS 273 CITATIONS

[SEE PROFILE](#)



Elise Fouquerel

University of Pittsburgh

11 PUBLICATIONS 132 CITATIONS

[SEE PROFILE](#)



Robert W Sobol

University of South Alabama

129 PUBLICATIONS 4,761 CITATIONS

[SEE PROFILE](#)



Barry Gold

University of Pittsburgh

142 PUBLICATIONS 2,639 CITATIONS

[SEE PROFILE](#)

## <sup>1</sup> Synthesis and Characterization of DNA Minor Groove Binding Alkylating Agents

<sup>3</sup> Prema Iyer,<sup>†</sup> Ajay Srinivasan,<sup>†</sup> Sreelekha K. Singh,<sup>†</sup> Gerard P. Mascara,<sup>†</sup> Sevara Zayitova,<sup>†</sup> Brian Sidone,<sup>†</sup>  
<sup>4</sup> Elise Fouquerel,<sup>‡</sup> David Svilar,<sup>‡,§,§</sup> Robert W. Sobol,<sup>‡,§,||</sup> Michael S. Bobola,<sup>⊥</sup> John R. Silber,<sup>⊥</sup>  
<sup>5</sup> and Barry Gold\*,<sup>†</sup>

<sup>6</sup> <sup>†</sup>Department of Pharmaceutical Sciences, University of Pittsburgh, Pittsburgh, Pennsylvania 15261, United States

<sup>7</sup> <sup>‡</sup>University of Pittsburgh Cancer Institute, University of Pittsburgh, Pittsburgh Pennsylvania 15232, United States

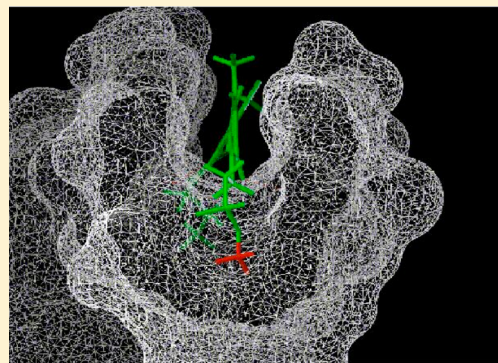
<sup>8</sup> <sup>§</sup>Department of Pharmacology & Chemical Biology, University of Pittsburgh, Pittsburgh, Pennsylvania 15261, United States

<sup>9</sup> <sup>||</sup>Department of Human Genetics, University of Pittsburgh, Pennsylvania 15213, United States

<sup>10</sup> <sup>⊥</sup>Department of Neurological Surgery, University of Washington, Seattle, Washington 98105, United States

### 11 Supporting Information

**ABSTRACT:** Derivatives of methyl 3-(1-methyl-5-(1-methyl-5-(propylcarbamoyl)-1*H*-pyrrol-3-ylcarbamoyl)-1*H*-pyrrol-3-ylamino)-3-oxopropane-1-sulfonate (**1**), a peptide-based DNA minor groove binding methylation agent, were synthesized and characterized. In all cases, the N-terminus was appended with an O-methyl sulfonate ester, while the C-terminus group was varied with nonpolar and polar side chains. In addition, the number of pyrrole rings was varied from 2 (dipeptide) to 3 (tri peptide). The ability of the different analogues to efficiently generate N3-methyladenine was demonstrated as was their selectivity for minor groove (N3-methyladenine) versus major groove (N7-methylguanine) methylation. Induced circular dichroism studies were used to measure the DNA equilibrium binding properties of the stable sulfone analogues; the tripeptide binds with affinity that is >10-fold higher than that of the dipeptide. The toxicities of the compounds were evaluated in *alkA/tag* glycosylase mutant *E. coli* and in human WT glioma cells and in cells overexpressing and under-expressing N-methylpurine-DNA glycosylase, which excises N3-methyladenine from DNA. The results show that equilibrium binding correlates with the levels of N3-methyladenine produced and cellular toxicity. The toxicity of **1** was inversely related to the expression of MPG in both the bacterial and mammalian cell lines. The enhanced toxicity parallels the reduced activation of PARP and the diminished rate of formation of aldehyde reactive sites observed in the MPG knockdown cells. It is proposed that unrepaired N3-methyladenine is toxic due to its ability to directly block DNA polymerization.



### 31 ■ INTRODUCTION

DNA damaging agents, which affect DNA metabolism,<sup>1</sup> continue to be extensively used in the treatment of cancer.<sup>1</sup> While interference with DNA metabolism causes cell death by apoptosis and/or necrosis, some cells survive through error free repair or error prone bypass of the lesion. The latter gives rise to increased mutations associated with higher cancer risk, and many of these DNA damaging drugs are listed by the International Agency for Cancer Research as human carcinogens.<sup>2</sup> In fact, there is significant incidence of secondary cancers that are directly attributable to the treatment of patients with antineoplastic agents for their primary cancer.<sup>3–6</sup> Because DNA remains a chemotherapeutic target for many cancers, it is important to minimize mutagenic side effects. In addition, new agents whose mechanisms of action do not overlap with existing therapies, including those that react with DNA,<sup>7–12</sup>

We previously developed alkylating agents related to netropsin that equilibrium bind to and efficiently react with

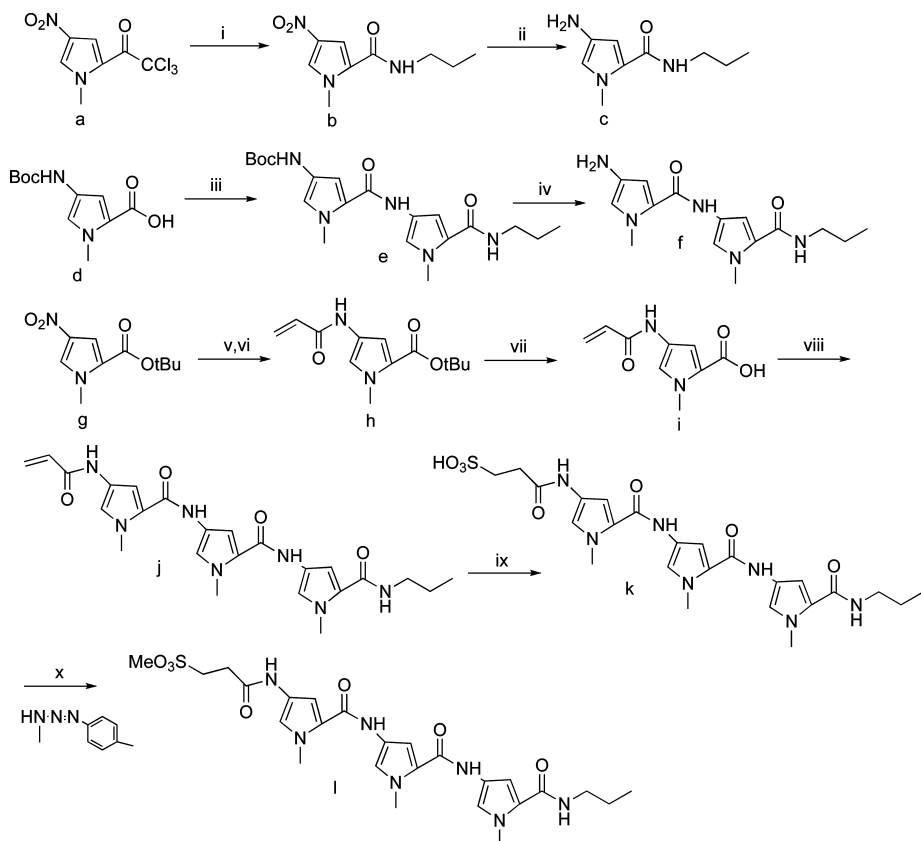
atoms that line the floor of the minor groove of DNA at A/T rich sequences, specifically the N3-position of adenine.<sup>13–17</sup> An O-methyl sulfonate ester was appended to the N-terminus of a *N*-methylpyrrolecarboxamide-based dipeptide to combine the alkylating activity with DNA equilibrium binding (Figure 1, compound **1**).<sup>13</sup> The C-terminus of the dipeptide was capped with an *n*-propyl group, thereby making the molecules neutral, unlike most natural product minor groove binders, which are cationic. The result is a DNA equilibrium binder with relatively weak affinity for DNA.<sup>18</sup> Despite this weak affinity due to the absence of stabilizing electrostatic interactions, the molecule efficiently and selectively reacts both in vitro and in cells to yield N3-methyladenine (3-mA).<sup>13–18</sup> Compound **1** is quite cytotoxic as compared to nonequilibrium binding alkylating agents, e.g., methyl methanesulfonate (MMS), and is relatively nonmutagenic.<sup>19–22</sup> In vitro data indicated that the toxicity

Received: October 29, 2012

compound	n	R <sub>1</sub>	R <sub>2</sub>
<b>1</b>	2	CH <sub>3</sub> O-	-CH <sub>2</sub> CH <sub>2</sub> CH <sub>3</sub>
<b>2</b>	2	CH <sub>3</sub> O-	-CH <sub>2</sub> CH=CH <sub>2</sub>
<b>3</b>	2	CH <sub>3</sub> O-	-CH <sub>2</sub> CH <sub>2</sub> OCH <sub>3</sub>
<b>4</b>	2	CH <sub>3</sub> O-	-CH <sub>2</sub> CH <sub>2</sub> OCH <sub>2</sub> CH <sub>2</sub> OCH <sub>3</sub>
<b>5</b>	2	CH <sub>3</sub>	-CH <sub>2</sub> CH <sub>2</sub> CH <sub>3</sub>
<b>6</b>	2	CH <sub>3</sub> -	-CH <sub>2</sub> CH=CH <sub>2</sub>
<b>7</b>	3	CH <sub>3</sub> O-	-CH <sub>2</sub> CH <sub>2</sub> CH <sub>3</sub>
<b>8</b>	3	CH <sub>3</sub> O-	-CH <sub>2</sub> CH=CH <sub>2</sub>
<b>9</b>	3	CH <sub>3</sub> O-	-CH <sub>2</sub> CH <sub>2</sub> OCH <sub>3</sub>
<b>10</b>	3	CH <sub>3</sub> -	-CH <sub>2</sub> CH <sub>2</sub> CH <sub>3</sub>
<b>11</b>	3	CH <sub>3</sub> -	-CH <sub>2</sub> CH=CH <sub>2</sub>
netropsin	2	NH <sub>2</sub> (NH=C)NHCH <sub>2</sub> -	-CH <sub>2</sub> CH <sub>2</sub> C(=NH)NH <sub>2</sub>
distamycin	3	H	-CH <sub>2</sub> CH <sub>2</sub> C(=NH)NH <sub>2</sub>

**Figure 1.** Structures of compounds.

**Scheme 1<sup>a</sup>**



<sup>a</sup>Reagents and conditions: (i) n-PrNH<sub>2</sub>, EtOAc; (ii) 10% Pd/C, EtOH; (iii) compound c, EDC, HOBT, Et<sub>3</sub>N, CH<sub>2</sub>Cl<sub>2</sub>; (iv) TFA, CH<sub>2</sub>Cl<sub>2</sub>; (v) 10% Pd/C, MeOH; (vi) CH<sub>2</sub>=CHCOCl, DIEA, THF; (vii) 1M TiCl<sub>4</sub>, CH<sub>2</sub>Cl<sub>2</sub>; (viii) compound f, EDC, HOBT, Et<sub>3</sub>N; (ix) NaHSO<sub>3</sub>, EtOH/H<sub>2</sub>O; (x) dioxane, 80 °C.

<sup>66</sup> results from the 3-mA lesion efficiently blocking DNA  
<sup>67</sup> replication and causing cell death.<sup>23-26</sup> In fact, the weak  
<sup>68</sup> mutagenicity of **1** was attributable to the intermediate  
<sup>69</sup> formation of abasic sites as part of the base excision repair  
<sup>70</sup> (BER) of 3-mA.<sup>27</sup>

We describe herein the synthesis and characterization of derivatives of dipeptide **1** with different C-termini and with an additional peptide subunit and analyze how these changes affect DNA methylation, affinity binding, and toxicity. To further explore the mechanism of toxicity of these compounds that generate 3-mA, we performed studies using cells that are WT for the human methylpurine DNA glycosylase (MPG), cells that overexpress MPG (MPG+), and cells where MPG has

been knocked down (MPG-). The time course for the formation of abasic sites and strand breaks with 5-p-dR termini, PARP activation, PARP inactivation, and caspase-3 and -7 activation were monitored. In addition, microfluidic assisted replication tract analysis was used to demonstrate that 3-mA directly or indirectly causes replication fork arrest in cells. The results provide new insights into the role of different BER intermediates and repair processes in cytotoxicity.

## ■ EXPERIMENTAL PROCEDURES

**Materials and Reagents.** *E. coli* AB1157 (WT) and *E. coli* 88-  
GC4803 (AlkA/tag) were obtained from T. O'Connor (City of Hope 88-  
National Medical Center, Duarte, CA) and L. Samson (Massachusetts 90-

91 Institute of Technology, Cambridge, MA). Human glioblastoma  
 92 (T98G) cells were obtained from American Type Culture Collection  
 93 (Manassas, VA). CellTiter 96 Aqueous One Solution Reagent was  
 94 obtained from Promega Corp (Madison, WI). T98G cells over-  
 95 expressing human MPG were developed essentially as described  
 96 previously by plasmid transfection.<sup>28,29</sup> Briefly,  $1.5 \times 10^5$  cells were  
 97 seeded into 60 mm dishes and incubated for 24–30 h at 5% CO<sub>2</sub> at 37  
 98 °C. The human MPG expression plasmid (pCMV-MPG-IRES-Neo)  
 99 was transfected using FuGene 6 Transfection Reagent (Roche;  
 100 Indianapolis, IN) according to the manufacturer's instructions. Stable  
 101 cell lines were selected in G418 for 2 weeks, and expression of human  
 102 MPG protein (nuclear extract) was validated by immunoblot analysis  
 103 and by activity analysis, as described.<sup>30,31</sup> The MPG– cells were  
 104 developed by shRNA-mediated gene knockdown using lentivirus  
 105 expressing MPG-specific shRNA.<sup>32</sup> The shRNA vectors used for stable  
 106 knockdown cell line development were obtained as glycerol stocks  
 107 from Sigma-Aldrich and the UPCI Lentiviral core facility (<http://www.upci.upmc.edu/vcf/lenti.cfm>). Lentiviral particles were generated  
 109 (in collaboration with the UPCI Lentiviral facility) by the  
 110 cotransfection of 4 plasmids [the shuttle vector plus three packaging  
 111 plasmids: pMD2-g(VSVG), pVSV-REV, and PMDLg/pRRE] into  
 112 293-FT cells using FuGene 6 Transfection Reagent (Roche,  
 113 Indianapolis, IN), as described previously.<sup>28</sup> Lentiviral transduction  
 114 was performed as described earlier.<sup>28</sup> Briefly,  $6.0 \times 10^4$  cells were  
 115 seeded into a 6-well plate 24 h before transduction. Cells were  
 116 transduced for 18 h at 32 °C and then cultured for 72 h at 37 °C. Cells  
 117 were then selected by culturing in growth media with 1.0 µg/mL  
 118 puromycin, as previously described.<sup>32</sup>

119 The DNA Damage Quantification kit (abasic site counting) was  
 120 purchased from Dojindo Molecular Technologies (Rockville, MD).  
 121 HT Colorimetric PARP Apoptosis Assay Kit was purchased from  
 122 Trevigen (Gaithersburg, MD). Pierce Cleaved PARP Colorimetric in-  
 123 cell ELISA kit was purchased from Thermo Scientific (Rockford, IL).  
 124 DNazol reagent, all cell culture components, Enzcheck Caspase-3  
 125 Assay kit, and Alexa Fluor 488 annexin V/Dead Cell Apoptosis Kit  
 126 were purchased from Invitrogen (Carlsbad, CA). Chemicals and  
 127 solvents were purchased from Sigma Aldrich Chemicals (St. Louis,  
 128 MO). 10%Pd–C was purchased from Strem chemicals. Molecular  
 129 biology grade buffers as well as plastic- and glass-ware were obtained  
 130 from Fisher Scientific (Pittsburgh, PA).

131 **Synthesis of DNA Methylating Agent 7.** See Scheme 1 and  
 132 Supporting Information for the synthesis and characterization of all  
 133 compounds. All <sup>1</sup>H NMR spectra were collected on a Bruker  
 134 instrument operating at 400 MHz, and data are reported as ppm.

135 **2,2,2-Trichloro-1-(1-methyl-4-nitro-1*H*-pyrrol-2-yl)ethanone.**  
 136 Compound (*a*) was prepared as previously described.<sup>33</sup>

137 **1-Methyl-4-nitro-N-propyl-1*H*-pyrrole-2-carboxamide (b).**  
 138 To a solution of *a* (3.47 g, 12.78 mmol) in 96 mL of EtOAc was  
 139 added propylamine (31.95 mmol, 2.6 mL) dropwise at 0 °C. The  
 140 reaction mixture was stirred for an additional 1 h and the solvent  
 141 evaporated to give *b* in 98% yield. <sup>1</sup>H NMR (CDCl<sub>3</sub>): δ 0.98 (t, 3H, J  
 142 = 7.3), 1.57–1.66 (m, 2H), 3.33–3.38 (m, 2H), 3.99 (s, 3H), 5.97 (s,  
 143 br, 1H), 7.04 (d, 1H, J = 1.83), 7.55 (d, 1H, J = 1.83).

144 **4-Amino-1-methyl-N-propyl-1*H*-pyrrole-2-carboxamide (c).**  
 145 To a solution of *b* (1g, 4.73 mmol) in EtOH (300 mL) was added  
 146 10% Pd/C catalyst (300 mg) and the reaction shaken in a Parr  
 147 apparatus at 50 psi until the disappearance of starting material (based  
 148 on TLC). The reaction mixture was filtered through a Celite pad and  
 149 solvents evaporated to dryness to give quantitative yields of *c*. <sup>1</sup>H  
 150 NMR (DMSO-*d*<sub>6</sub>) δ 0.84 (t, 3H, J = 7.42), 1.42–1.48 (m, 2H), 3.05–  
 151 3.09 (m, 2H), 3.66 (s, 3H), 6.16 (d, 1H, J = 1.95), 6.17 (d, 1H, J =  
 152 1.95), 7.70 (t, 1H, J = 5.47).

153 **4-((t-Butoxycarbonyl)amino)-1-methyl-1*H*-pyrrole-2-carbox-  
 154 ylic Acid (d).** The title compound was prepared as previously  
 155 reported.<sup>33</sup>

156 **t-Butyl(1-methyl-5-((1-methyl-5-(propylcarbamoyl)-1*H*-pyr-  
 157 rol-3-yl)carbamoyl)-1*H*-pyrrol-3-yl)carbamate (e).** To a solution  
 158 of *d* (538 mg, 2.24 mmol) and HOBT (454 mg, 3.36 mmol) in  
 159 anhydrous CH<sub>2</sub>Cl<sub>2</sub> (30 mL) was added Et<sub>3</sub>N (1.25 mL, 8.96 mmol)  
 160 and EDC (859 mg, 4.48 mmol). The reaction mixture was stirred at

room temperature for 1 h under N<sub>2</sub>. After 1 h, the reaction mixture  
 161 was cooled, and amine *c* (609 mg, 3.36 mmol) was added in CH<sub>2</sub>Cl<sub>2</sub>  
 162 (20 mL) containing Et<sub>3</sub>N (500 µL). The reaction mixture was stirred  
 163 under N<sub>2</sub> for 18 h and then diluted with CH<sub>2</sub>Cl<sub>2</sub> and washed with  
 164 H<sub>2</sub>O. The aqueous layer was extracted with CH<sub>2</sub>Cl<sub>2</sub>, dried over  
 165 Na<sub>2</sub>SO<sub>4</sub>, and the solvent evaporated. The residue was purified by silica  
 166 gel column chromatography to obtain *e* in 86% yield. <sup>1</sup>H NMR  
 167 (DMSO-*d*<sub>6</sub>) δ 0.86 (t, 3H, J = 7.42), 1.45 (s, 9H), 1.46–1.52 (m, 2H),  
 168 3.09–3.14 (m, 2H), 3.78 (s, 3H), 3.79 (s, 3H), 6.81 (s, br, 1H), 6.84  
 169 (d, 1H, J = 1.56), 6.88 (s, br, 1H), 7.15 (d, 1H, J = 1.95), 7.98 (t, 1H, J  
 170 = 5.46), 9.09 (s, 1H), 9.80 (s, 1H).  
 171

172 **4-Amino-1-methyl-N-(1-methyl-5-(propylcarbamoyl)-1*H*-  
 173 pyrrol-3-yl)-1*H*-pyrrole-2-carboxamide (f).** To a solution of *e*  
 174 (671 mg, 1.66 mmol) in anhydrous CH<sub>2</sub>Cl<sub>2</sub> (8 mL) was added 50%  
 175 TFA/CH<sub>2</sub>Cl<sub>2</sub> (v/v, 24 mL) at 0 °C such that the final concentration of  
 176 TFA is approximately 40%. The reaction mixture was stirred at 0 °C  
 177 until the complete disappearance of starting material (based on TLC).  
 178 The solvent was evaporated to dryness to give *f* in quantitative yield.  
 179 <sup>1</sup>H NMR (DMSO-*d*<sub>6</sub>) δ 0.86 (t, 3H, J = 7.42), 1.44–1.539 m, 2H),  
 180 3.09–3.15 (m, 2H), 3.80 (s, 3H), 3.89 (s, 3H), 6.84 (d, 1H, J = 1.95),  
 181 6.94 (d, 1H, J = 1.95), 7.11 (d, 1H, J = 1.95), 7.18 (d, 1H, J = 1.95),  
 182 8.01 (t, 1H, J = 5.46), 9.75 (s, 1H), 9.98 (s, 1H).  
 183

184 **t-Butyl 1-Methyl-4-nitro-1*H*-pyrrole-2-carboxylate (g).** The  
 185 title compound was prepared as previously described.<sup>34</sup>  
 186

187 **t-Butyl 4-Acylamido-1-methyl-1*H*-pyrrole-2-carboxylate (h).** To a solution of *g* (1.4 g, 6.19 mmol) in MeOH (350 mL) was  
 188 added 10% Pd/C catalyst (1 g) and the reaction mixture shaken in a  
 189 Parr apparatus at 55 psi until the complete disappearance of starting  
 190 material (by TLC). The reaction mixture was filtered through a Celite  
 191 pad and solvents evaporated to dryness to afford the amine in  
 192 quantitative yield (1.06 g, 5.40 mmol), which was dissolved in  
 193 anhydrous THF (70 mL) and DIEA (2.8 mL, 16.20 mmol). The  
 194 reaction mixture was cooled to –78 °C, and acryloyl chloride (658 µL,  
 195 8.10 mmol) was added dropwise. The reaction mixture was maintained  
 196 at –78 °C until the disappearance of the amine was complete (based  
 197 on TLC). The THF was concentrated to a minimum volume and  
 198 diluted with CH<sub>2</sub>Cl<sub>2</sub> and washed with H<sub>2</sub>O. The aqueous layer was  
 199 extracted thoroughly with CH<sub>2</sub>Cl<sub>2</sub>, dried over Na<sub>2</sub>SO<sub>4</sub>, and solvents  
 200 evaporated to dryness. The residue was purified by silica gel column  
 201 chromatography to yield *h* in 76% yield. <sup>1</sup>H NMR (DMSO-*d*<sub>6</sub>) δ 1.49  
 202 (s, 9H), 3.79 (s, 3H), 5.67 (dd, 1H, J = 10.16 and 2.34), 6.16 (dd, 1H, J  
 203 = 17.19, and 2.34), 6.27–6.34 (m, 1H), 6.71 (d, 1H, J = 1.95), 7.34 (d,  
 204 1H, J = 1.95), 10.08 (s, br, 1H).  
 205

206 **4-Acylamido-1-methyl-1*H*-pyrrole-2-carboxylic Acid (i).** To a  
 207 solution of *h* (1.032 g, 4.12 mmol) in CH<sub>2</sub>Cl<sub>2</sub> (30 mL) was added 1  
 208 M TiCl<sub>4</sub> solution (10 mL, 10.31 mmol) at 0 °C. The reaction mixture  
 209 was stirred and slowly allowed to come to room temperature until the  
 210 complete disappearance of starting material. The reaction mixture was  
 211 diluted with CH<sub>2</sub>Cl<sub>2</sub> and washed with H<sub>2</sub>O. The aqueous layer was  
 212 extracted with EtOAc and the organic solvent extracts pooled, dried  
 213 over Na<sub>2</sub>SO<sub>4</sub>, and evaporated to dryness to yield 96% of *i*. <sup>1</sup>H NMR  
 214 (DMSO-*d*<sub>6</sub>) δ 3.81 (s, 3H), 5.67 (dd, 1H, J = 9.77 and 1.96), 6.17 (dd,  
 215 1H, J = 17.18 and 1.96), 6.29–6.35 (m, 1H), 6.71 (d, 1H, J = 1.95),  
 216 7.38 (d, 1H, J = 1.95), 10.09 (s, br, 1H), 12.22 (s, br, 1H).  
 217

218 **4-Acylamido-1-methyl-N-(1-methyl-5-((1-methyl-5-(propyl-  
 219 carbamoyl)-1*H*-pyrrol-3-yl)carbamoyl)-1*H*-pyrrol-3-yl)-1*H*-pyr-  
 220 role-2-carboxamide (j).** To a solution of *i* (217 mg, 1.12 mmol) and  
 221 HOBT (225 mg, 1.66 mmol) in anhydrous CH<sub>2</sub>Cl<sub>2</sub> (20 mL) was  
 222 added Et<sub>3</sub>N (0.618 mL, 4.44 mmol) and EDC (425 mg, 2.22 mmol).  
 223 The reaction mixture was stirred at room temperature for 1 h under  
 224 N<sub>2</sub>, cooled, and amine *f* (505 mg, 1.66 mmol) added in CH<sub>2</sub>Cl<sub>2</sub> (11  
 225 mL) containing Et<sub>3</sub>N (1 mL). The reaction mixture was stirred under  
 226 N<sub>2</sub> for 18 h and then diluted with CH<sub>2</sub>Cl<sub>2</sub> and washed with H<sub>2</sub>O. The  
 227 aqueous layer was extracted thoroughly with CH<sub>2</sub>Cl<sub>2</sub>, dried over  
 228 Na<sub>2</sub>SO<sub>4</sub>, and solvents evaporated. The residue was purified by silica gel  
 229 column chromatography to afford *j* in 60% yield. <sup>1</sup>H NMR (DMSO-  
 230 *d*<sub>6</sub>) δ 0.87 (t, 3H), 1.46–1.52 (m, 2H), 3.10–3.16 (m, 2H), 3.79 (s,  
 231 3H), 3.84 (s, 3H), 3.85 (s, 3H), 5.67 (dd, 1H, J = 10.15 and 1.95),  
 232 6.19 (dd, 1H, J = 17.19 and 1.95), 6.34–6.41 (m, 1H), 6.86 (d, 1H, J =  
 233 1.56), 6.94 (d, 1H, J = 1.56), 7.04 (d, 1H, J = 1.95), 7.18 (d, 1H, J =  
 234 1.56), 7.22 (s, 1H).  
 235

231 1.95), 7.25 (d, 1H,  $J$  = 1.95), 7.28 (d, 1H,  $J$  = 1.95), 8.0 (t, 1H,  $J$  =  
232 5.47), 9.89 (s, 1H), 9.95 (s, 1H), 10.12 (s, 1H).

233 **3-((1-Methyl-5-((1-methyl-5-((propylcarbamoyl)-1H-pyrrol-3-yl)carbamoyl)-1H-pyrrol-3-yl)amino)-3-oxopropane-1-sulfonic Acid (k).** To a  
234 solution of *j* (123 mg, 0.257 mmol) in EtOH/H<sub>2</sub>O (4:1, 5.6 mL)  
235 was added NaHSO<sub>3</sub> solution (0.514 mmol, 55 mg in 0.740 mL H<sub>2</sub>O).  
236 The pH of the solution was adjusted to 8 and the reaction mixture  
237 refluxed at 90 °C until the complete disappearance of starting material  
238 (based on TLC). The reaction was cooled to 0 °C, and concd HCl was  
239 added dropwise so that the pH was between 1 and 2. The solvent was  
240 evaporated to dryness to yield a bright yellow solid that was treated  
241 with cold 2 N HCl. The mixture was centrifuged (4000 rpm, 10 min)  
242 and the supernatant decanted off, and the remaining solid was twice  
243 washed again with 2 N cold HCl, centrifuged, and the supernatant  
244 decanted. The remaining solid material was thoroughly dried to give  
245 93% of **k**. <sup>1</sup>H NMR (DMSO-*d*<sub>6</sub>)  $\delta$  0.87 (t, 3H), 1.44–1.53 (m, 2H),  
246 2.53–2.57 (m, 2H), 2.66–2.70 (m, 2H), 3.09–3.15 (m, 2H), 3.79 (s,  
247 3H), 3.83 (s, 3H), 3.84 (s, 3H), 6.85 (d, 1H,  $J$  = 1.56), 6.87 (d, 1H,  $J$  =  
248 1.56), 7.03 (d, 1H,  $J$  = 1.95), 7.15 (d, 1H,  $J$  = 1.56), 7.18 (d, 1H,  $J$  =  
249 1.95), 7.24 (d, 1H,  $J$  = 1.56), 8.0 (t, 1H,  $J$  = 6.48), 9.89 (s, 1H), 9.91 (s,  
250 1H), 9.97 (s, 1H).

251 **Methyl 3-(1-Methyl-5-(1-methyl-5-(1-methyl-5-(propylcarbamoyl)-1H-pyrrol-3-yl)carbamoyl)-1H-pyrrol-3-yl)-3-carbamoyl)-1H-pyrrol-3-ylamino)-3-oxopropane-1-sulfonate (l).** To a solution of **k** (129 mg, 0.229 mmol) in dry dioxane (13 mL)  
252 was added 3-methyl-1-*p*-tolyltriaz-1-ene (343 mg, 2.297 mmol). The  
253 reaction was heated in an oil bath at 80 °C for ~4 h. The dioxane was  
254 reduced to minimum volume and the residue loaded onto a Et<sub>3</sub>N  
255 deactivated silica gel column. The product **l** (49%) was eluted with  
256 EtOAc. <sup>1</sup>H NMR (DMSO-*d*<sub>6</sub>)  $\delta$  0.87 (t, 3H), 1.46–1.52 (m, 2H), 2.74  
257 (t, 2H,  $J$  = 7.42), 3.10–3.15 (m, 2H), 3.62 (t, 2H,  $J$  = 7.42), 3.79 (s,  
258 3H), 3.84 (s, br, 6H), 3.87 (s, 3H), 6.86 (d, 1H,  $J$  = 1.57), 6.89 (d, 1H,  
259  $J$  = 1.95), 7.03 (d, 1H,  $J$  = 1.95), 7.16–7.19 (m, 2H), 7.24 (d, 1H,  $J$  =  
260 1.95), 8.0 (t, 1H,  $J$  = 5.08), 9.89 (s, 1H), 9.93 (s, 1H), 10.07 (s, 1H).  
261 <sup>13</sup>C NMR (150 MHz, DMSO-*d*<sub>6</sub>) 11.94, 23.08, 29.86, 36.39, 36.60,  
262 36.64, 40.66, 44.50, 57.45, 104.39, 104.55, 105.12, 118.14, 118.67,  
263 118.92, 122.12, 122.53, 122.55, 123.24, 123.33, 123.56, 158.82, 158.91,  
264 161.70, 166.05. HR-MS (ES + H) *m/z*: calcd for C<sub>25</sub>H<sub>34</sub>N<sub>7</sub>O<sub>7</sub>S,  
265 (576.2240). Found: (576.2261).

266 **DNA Equilibrium Binding Studies.** Calf thymus DNA (CT-  
267 DNA), poly (deoxyadenylic–thymidylic) acid sodium salt [poly d(A-  
268 T)], netropsin, and distamycin were purchased from Sigma-Aldrich, St.  
269 Louis, MO. The stock solutions for these polymers were prepared by  
270 overnight dialysis at 4 °C against 10 mM sodium phosphate buffer  
271 containing 1 mM Na<sub>2</sub>EDTA and 10% EtOH at pH 7. The  
272 concentration of stock CT-DNA and poly d(A-T) solutions were  
273 measured on a UV spectrophotometer using their extinction  
274 coefficient as  $\epsilon_{260}$  = 6550 M<sup>-1</sup> cm<sup>-1</sup> and  $\epsilon_{260}$  = 6500 M<sup>-1</sup> cm<sup>-1</sup>,  
275 respectively. For all the experimental purposes, the compounds were  
276 dissolved in the respective buffers and their concentrations determined  
277 spectrophotometrically using the extinction coefficients,  $\epsilon_{296}$  = 21,500  
278 M<sup>-1</sup> cm<sup>-1</sup> for **5**, **6**, and netropsin, and  $\epsilon_{303}$  = 34,000 M<sup>-1</sup> cm<sup>-1</sup> for **10**,  
279 **11**, and distamycin.

280 Thermal denaturation experiments were carried out on a Cary UV  
281 300 Bio UV-visible spectrophotometer (Varian Inc., Palo Alto, CA)  
282 coupled to a Cary Temperature Controller unit. All the experiments  
283 were performed using a 1.4 mL cuvette (1 cm path length). The  
284 melting of CT-DNA and poly d(A-T) were monitored at 260 and 275  
285 nm in the temperature range of 0–95 °C at a heating rate of 0.5 °C/  
286 min with a data interval of 0.2 °C in the absence and presence of  
287 sulfones **5**, **6**, **10**, and **11**. The melting temperature (*T<sub>M</sub>*) was  
288 determined by the analysis of the shape and first-derivative of the  
289 melting curves.

290 The induced circular dichroism (ICD) titration of compounds **5**, **6**,  
291 **10**, and **11** with CT-DNA and poly d(A-T) were performed on a  
292 Jasco-815 CD spectrometer (Jasco Corporation, Tokyo, Japan)  
293 equipped with a Jasco PTC-423S/15 Peltier Temperature Controller  
294 system. Two-point calibration of the CD spectrometer was checked  
295 using 3.855 mM (1S)-(+)-10-camphorsulphonic acid. The spectra of

296 this solution in a 1 mm cuvette resulted in the ratio  $\epsilon_{191}/\epsilon_{291} = -2.00$ .  
297 All the experiments were done at a constant temperature of 20 °C  
298 maintained with the help of Julabo F25-ME refrigerated/heating  
299 circulator. The spectrometer was purged for ~15 min with N<sub>2</sub> before  
300 starting the instrument and then ~30 min for the light source to attain  
301 stability before starting the experiments. The serial dilution approach  
302 to ICD described by Garbett et al.<sup>35</sup> was used to titrate the sulfone  
303 compounds (~10–50 μM) with CT-DNA or poly d(A-T) in the  
304 concentration range of 1 nM to 1 mM. In this approach, an experiment  
305 was started with a solution containing the maximum concentration of  
306 the DNA substrate and then serially diluting the solution in the cuvette  
307 with a ligand stock solution of the same concentration as in the cuvette  
308 to achieve the required concentration range of the DNA substrate,  
309 thus titrating the DNA substrate against a constant ligand  
310 concentration. A semimicrocuvette with nontransmitting black walls  
311 with a 1 cm path length was used for all the experiments. The spectra  
312 were scanned from 400 to 220 nm with a data pitch of 0.1 nm and a  
313 scan speed of 100 nm/min with 1 s response time and 1 nm  
314 bandwidth. Each spectrum was buffer subtracted and the final plot  
315 taken as an average of three accumulated scans. The binding curve was  
316 obtained by plotting the maxima of the induced CD signal of the  
317 sulfone compounds as a function of the logarithm of the DNA  
318 substrate concentration. The binding constant was calculated by  
319 evaluating the slope of the graph using the nonlinear fit option in  
320 Origin/FitAll software as previously described.<sup>35</sup>

321 **DNA Methylation.** CT DNA (100 μM, nucleotide), dialyzed  
322 overnight against 10 mM sodium cacodylate buffer (pH 7.0) was  
323 reacted at room temperature for 24 h with methylvating compounds  
324 (dissolved in minimal volume of ice-cold 95% EtOH) at final  
325 concentrations of 1, 5, 10, and 100 μM in 10 mM sodium cacodylate  
326 buffer (pH 7.0) in a total volume of 2 mL (for 1, 5, and 10 μM  
327 alkylating agent) or 1 mL (for 100 μM alkylating agent). The DNA  
328 was precipitated from the reaction solution with 3 M NaOAc (pH 4.8)  
329 and EtOH, and then redissolved in 10 mM sodium cacodylate buffer  
330 (pH 7.0) to a total volume of 500 μL and heated for 30 min at 90 °C  
331 to release N3- and N7-alkylpurines. The partially apurinic DNA was  
332 precipitated at 0 °C by adding 50 μL of cold 0.1 N HCl. The  
333 supernatant containing the N-methylpurines was analyzed by HPLC.  
334 For the measurement of 3-mA, the following conditions were utilized:  
335 column, Partisil 10 SCX; temperature, 25 °C; eluent, 175 mM  
336 ammonium formate (pH 3.0) containing 30% (v/v) MeOH; flow rate,  
337 1 mL/min; detection, UV at 270 nm. For simultaneous measurement  
338 of both 3-mA and 7-methylguanine (7-mG), the following conditions  
339 were utilized: Syngeri Fusion-RP column (temperature, 25 °C; eluent,  
340 50 μM ammonium formate (pH 4.0) containing 2% (v/v)  
341 isopropanol; flow rate, 1.25 mL/min; detection, UV at 270 and 280  
342 nm). Authentic standards of 3-mA and 7-mG were used for HPLC  
343 identification of adducts and to calculate response factors.

344 **E. coli Cytotoxicity Assays.** Cultures of *Escherichia coli* strains  
345 AB1157 (str<sup>r</sup>, wild type) and GC4803 (alk<sup>-/-</sup> tag<sup>-/-</sup> kan<sup>r</sup>, DNA repair  
346 mutant) were started from frozen stocks, in liquid LB media with the  
347 corresponding antibiotic. Overnight cultures of the strains were used  
348 to seed 10 mL of LB medium and the cells allowed to grow for 2–3 h  
349 until they reached the midlog growth stage (OD<sub>600</sub> = 0.5). Cells were  
350 harvested from 1 mL aliquots by centrifugation (5000g, 5 min),  
351 washed with phosphate buffered saline (PBS) and resuspended in 950  
352 μL of PBS. Preweighed aliquots of compounds were dissolved in 95%  
353 EtOH to give a 1 M stock. Dilutions of this stock were used to confirm  
354 the concentration of compound in solution by UV absorbance.  
355 Depending on the observed concentration, the stock solution of  
356 alkylating agent was diluted in appropriate volumes of 95% EtOH to  
357 obtain working stocks of 40, 80, 120, 160, and 200 μM. Then, 50 μL of  
358 each stock solution was added to 950 μL of the previously prepared  
359 cell suspension (in 1× PBS) and mixed by vortexing. The cells were  
360 treated with the methylvating compounds for 1 h at 37 °C. A control  
361 set was included in which cells were treated similarly with 5% EtOH in  
362 1× PBS. Post-treatment, the cells were harvested by centrifugation,  
363 rinsed with 1× PBS, serially diluted (10<sup>0</sup>–10<sup>-6</sup>) in 1× PBS and plated  
364 on solid LB media with the appropriate antibiotic. After 16 h, colonies  
365

370 were counted on the plate, and cell viability (survival %) was calculated  
 371 relative to that of the control set.  
**372 T98G Glioma Cell Cytotoxicity Assay.** Human glioblastoma cells  
 373 (T98G) were maintained in growth medium, i.e., Eagle's Minimum  
 374 Essential Medium (EMEM) with 10% fetal bovine serum (FBS), 50  $\mu\text{g}$   
 375  $\mu\text{L}^{-1}$  gentamycin, 1× MEM nonessential amino acids, and 1 mM  
 376 sodium pyruvate. To evaluate short-term cytotoxicity measuring viable  
 377 cells, T98G cells maintained in growth medium were harvested by  
 378 trypsin-EDTA treatment and resuspended in fresh growth medium at  
 379 a density of  $10^4$  cells  $\text{mL}^{-1}$ , and 200  $\mu\text{L}$  ( $2 \times 10^3$  cells) of this  
 380 suspension was seeded into the wells of a sterile 96-well tissue culture  
 381 microplate. The cells were allowed to attach and grow for 24 h and  
 382 then treated with serial dilutions of the drug for 72 h. After treatment,  
 383 viable cells were measured using an MTS assay using the CellTiter 96  
 384 AQueous kit (Promega) as per the manufacturer's instructions. To  
 385 assay long-term cytotoxicity, cells were grown until approximately 50–  
 386 75% confluence before being trypsinized and counted using a CASY  
 387 counter per the manufacturer's instructions. Cells were seeded into 96-  
 388 well plates at a density of 120 cells/well and incubated at 37 °C for 24  
 389 h. The cells were treated with 1 and incubated for 9 days at 37 °C.  
 390 Plates were removed, and fluorescence was determined using the  
 391 CyQuant kit (Invitrogen, #C7026) following the manufacturer's  
 392 instructions. Results were the average of two separate experiments  
 393 and normalized to vehicle treated control cells with error bars  
 394 representing the standard error of the mean, as previously described.<sup>35</sup>

395 **Quantification of Aldehyde Reactive Sites (ARS).** T98G cells  
 396 maintained in growth medium were harvested by trypsin-EDTA  
 397 treatment and resuspended in fresh growth medium at a density of  $2.5$   
 398  $\times 10^5$  cells/mL, and 2 mL ( $5 \times 10^5$  cells) of this suspension was  
 399 seeded into the wells of a sterile 6-well tissue culture plate. Cells were  
 400 allowed to grow for 24 h, treated with the various compounds for  
 401 different time points and/or at different concentrations. At the end of  
 402 each treatment, adherent cells were harvested by trypsin-EDTA  
 403 treatment and pooled with cells in the culture supernatant. Pooled  
 404 cells in suspension were pelleted by centrifugation, washed with 1×  
 405 PBS and genomic DNA isolated using the DNAzol reagent  
 406 (Invitrogen). DNA in solution was quantified by UV absorbance at  
 407 260 nm using a Synergy H1 multiwell plate reader (BioTek, Winooski,  
 408 VT). ARS in purified DNA were then reacted with the biotin-  
 409 conjugated aldehyde reactive probe, immobilized onto 96-well ELISA  
 410 plates, and detected using horseradish peroxidase (HRP)-conjugated  
 411 streptavidin using a colorimetric substrate as per the manufacturer's  
 412 instructions (Dojindo Molecular Technologies, Rockville, Maryland).

413 **Markers of Apoptosis.** T98G cells maintained in growth medium  
 414 were harvested by trypsin-EDTA treatment, resuspended in fresh  
 415 growth medium, and seeded into 96- or 6-well plates as per the assay  
 416 requirements: (i) to measure PARP activity,  $2 \times 10^4$  cells were seeded  
 417 into the wells of a 96 well plate, (ii) to measure PARP cleavage,  $10^4$   
 418 cells were seeded into the wells of a 96-well plate, and (iii) to measure  
 419 caspase-3 and -7 activities,  $10^6$  cells were seeded into the wells of a 6-  
 420 well plate. Cells were allowed to grow for 24 h, treated with  
 421 compounds for different time periods and/or at different concen-  
 422 trations. At the end of each treatment, adherent cells were harvested  
 423 by trypsin-EDTA treatment and pooled with cells in the supernatant.  
 424 The PARP activity was determined by measuring the deposition of  
 425 PAR on immobilized histones using anti-PAR (primary antibody) and  
 426 horseradish peroxidase (HRP) conjugated secondary antibody  
 427 (Trevigen Inc., Gaithersburg, MD). PARP cleavage was measured  
 428 using anticleaved PARP (primary antibody) and HRP-conjugated  
 429 secondary antibody (Thermo Fisher Scientific, Pittsburgh, PA).  
 430 Intracellular caspase-3 and -7 activities were measured using Z-  
 431 DEVD-AMC (benzyloxycarbonyl-Asp-Glu-Val-Asp-7-amino-4-methyl-  
 432 coumarin), a synthetic fluorogenic substrate of cysteine proteases, such  
 433 as caspase-3 and -7 (Invitrogen, Carlsbad, CA).

434 **Microfluidic Assisted Replication Tract Analysis.** Human glial  
 435 SF767 tumor cells were incubated with 50  $\mu\text{M}$  iododeoxyuridine  
 436 (IdU) to label active replication forks.<sup>36</sup> After removal of IdU, cells  
 437 were incubated with 50  $\mu\text{M}$  chlorodeoxyuridine (CldU) in the  
 438 presence of solvent or **1** (5 or 10  $\mu\text{M}$ ). The DNA from the cells was  
 439 isolated and loaded into microcapillaries and immunostained with

440 antibodies specific for each of the halogenated pyrimidines. The  
 441 capillaries were examined under a fluorescent microscope equipped  
 442 with a digital camera to locate areas with optical density and alignment.  
 443 Each of the fields selected was photographed twice with different filters  
 444 to obtain 2 color images. Approximately 50–80 images were taken of  
 445 3–4 microchannels for each sample in order to collect 300–400  
 446 replication tracks. Track lengths were measured using AxioVision  
 447 image analysis software. The criteria for collecting image data on a  
 448 track were DNA density and track alignment; tracks containing 3  
 449 labeled segments (e.g., green-red-green) that likely present the  
 449 merging of forks from adjacent replicons were not included.  
 450

## ■ RESULTS

451 **Synthesis.** The syntheses of the sulfonate ester and sulfone  
 452 analogues of the di- and tripeptide minor groove binders with  
 453 the different C-terminus groups (Figure 1) generally followed  
 454 previously published procedures<sup>13</sup> with modifications that are  
 455 described in Experimental Procedures and in Supporting  
 456 Information.  
 457

458 **Methylation of DNA.** The yields of 3-mA as a result of  
 459 incubating different concentrations of compounds **1–4**, **7**, and  
 460 **8** with CT-DNA for 24 h at room temperature in pH 7.0  
 461 sodium cacodylate buffer are shown in Figure 2A. Among the 2-  
 462

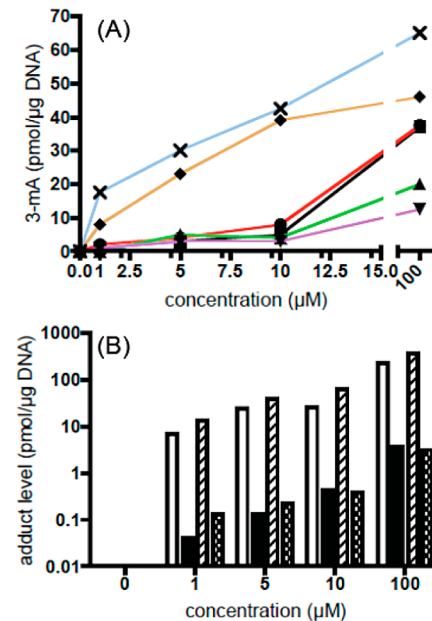


Figure 2. (A) Formation of N3-methyladenine (3-mA) from the 24 h incubation of calf thymus DNA (100  $\mu\text{M}$  nucleotide) with compounds **1–4**, **7**, and **8** at room temperature in 10 mM sodium cacodylate buffer (pH 7.0): **1** (■), **2** (●), **3** (▲), **4** (▼), **7** (◆), and **8** (✖). (B) Formation of 3-mA and N7-methylguanine (7-mG) from the incubation of **1** and **7** with calf thymus DNA in 10 mM cacodylate buffer (pH 7.0) at room temperature for 24 h.

463 ring compounds, the methoxyethyl (**3**) and methoxyethox-  
 464 yethyl (**4**) ethers yielded the lowest amount of 3-mA, although  
 465 the difference between any of the 2-ring compounds was only  
 466 evident at the highest (100  $\mu\text{M}$ ) concentration. It appears that  
 467 the compounds with more polar C-terminal side chains have  
 468 weaker methylating activity than those with the more  
 469 hydrophobic propyl and allyl groups. The tripeptide propyl  
 470 (**7**) and allyl (**8**) compounds show a clear concentration  
 471 response with 3-mA adduct being observed even at the 1  $\mu\text{M}$   
 472

**Table 1.** Minor (3-mA) and Major (7-mG) Groove Adduct Production (pmol/μg DNA) from the Reaction of **1** and **7** with CT-DNA<sup>a</sup>

concn compd	1 μM		5 μM		10 μM		100 μM	
	<b>1</b>	<b>7</b>	<b>1</b>	<b>7</b>	<b>1</b>	<b>7</b>	<b>1</b>	<b>7</b>
<b>3-mA</b>	7.15	13.11	24.36	38.04	25.55	62.08	232.14	365.27
<b>7-mA</b>	0.04	0.13	0.13	0.22	0.43	0.39	3.56	3.13
<b>3-mA/7-mG</b>	179	101	187	173	59	159	65	117

<sup>a</sup>Reactions conditions: 24 h incubation of compounds with CT-DNA (100 μM, p) at room temperature in 10 mM sodium phosphate buffer (pH 7.0). Data are based on HPLC analysis with UV detection.

471 concentration. Analogue **8** with the allyl terminus was the most  
472 active compound.

473 The preference of dipetide **1** and tripeptide **7** for minor  
474 groove versus major groove alkylation was assessed by  
475 comparing the relative yields of 3-mA and 7-mG (Figure 2B  
476 and Table 1). At the 1 and 5 μM concentrations, the ratio  
477 averages >100:1 minor over major groove for both compounds.  
478 At the 10 and 100 μM concentrations, the 3-mA to 7-mG ratio  
479 drops to approximately 60:1 for dipetide **1** but remains >100:1  
480 for tripeptide **7**. Therefore, DNA methylation by the two  
481 compounds is essentially restricted to the formation of 3-mA.  
482 This contrasts with the 1:10 3-mA to 7-mG ratio observed with  
483 MMS and related methylating agents.

484 **DNA Equilibrium Binding.** Several approaches were used  
485 to probe the relationship between DNA methylation by the  
486 different minor groove binders and their equilibrium binding to  
487 DNA using sulfone derivatives **5**, **6**, **10**, and **11**. The sulfonate  
488 esters are relatively reactive (*t*<sub>1/2</sub> of ~6 h in pH 7 buffer,  
489 Supporting Information) and are converted into the sulfonate  
490 anion after they transfer their methyl group to a nucleophile.  
491 The sulfones are isosteric, neutral, and stable in solution. Initial  
492 attempts to use isothermal titration calorimetry (ITC) was  
493 thwarted due to either limited solubility of the compounds in  
494 aqueous buffer systems and the low heat liberated upon  
495 binding.

496 **UV Melting Studies.** The UV extinction coefficient of  
497 DNA as a function of temperature is related to the thermal  
498 stability of duplex DNA. The effect of **5**, **6**, **10**, and **11** on the  
499 thermal stability of CT-DNA and poly-(dA-dT) was  
500 determined by monitoring absorbance at 260 nm and  
501 calculating the midpoint melting temperature (*T*<sub>M</sub>). Ligands  
502 that bind to double stranded DNA generally stabilize the duplex  
503 and increase the *T*<sub>M</sub>. A summary of the effect of the four  
504 compounds on the thermal stability of CT-DNA and poly d(A-  
505 T) is given in Table 2. The 2-ring compounds **5** and **6** showed  
506 a minimal increase in stability with a Δ*T*<sub>M</sub> of 0.4 °C for CT-  
507 DNA and 1.2 °C for poly d(A-T). The 3-ring compounds **10**  
508 and **11** were more stabilizing: Δ*T*<sub>M</sub> of 1.1 °C for **10** and 11 °C for **11** with poly  
509 d(A-T). In comparison, netropsin and distamycin raise the *T*<sub>M</sub>  
510 of CT-DNA by 21.1 and 17.0 °C, and of poly d(A-T) by 40.6  
511 and 36.9 °C, respectively.

512 **Induced CD Studies.** The 2- and 3-ring peptide  
513 compounds are achiral and optically inactive. However, upon  
514 interaction with DNA, ligands can acquire an induced-CD  
515 signal through the coupling of electric transition  
516 moments of the ligand and the chiral double helix. This  
517 induced Cotton effect is distinct from the DNA CD spectrum  
518 and directly reflects the ligand–DNA interaction.<sup>35</sup> The CD  
519 titration of netropsin, distamycin, and tripeptides **10** and **11**  
520 with CT-DNA and poly d(A-T) are represented in Figure 3 and  
521 the corresponding values for the binding constants are reported

**Table 2.** Thermodynamic Parameters for the Equilibrium Binding of Minor Groove Binding Methylsulfones to Calf Thymus (CT)-DNA and Poly-d(A-T)<sup>a</sup>

compd <sup>b</sup>	Δ <i>T</i> <sub>M</sub> (°C) <sup>c</sup>		K <sub>b</sub> (M <sup>-1</sup> ) <sup>d</sup>	
	CT-DNA	poly d(A-T)	CT-DNA	poly d(A-T)
<b>5</b>	0.4	1.2	n.d. <sup>e</sup>	n.d.
<b>6</b>	0.4	1.2	n.d.	n.d.
<b>10</b>	1.1	4.1	2.9 × 10 <sup>4</sup>	2.0 × 10 <sup>4</sup>
<b>11</b>	1.1	4.7	3.2 × 10 <sup>4</sup>	1.8 × 10 <sup>4</sup>
netropsin	21.1	40.6	2.0 × 10 <sup>5</sup>	2.4 × 10 <sup>5</sup>
distamycin	17.0	36.9	2.1 × 10 <sup>5</sup>	5.1 × 10 <sup>5</sup>

<sup>a</sup>All analyses were performed in 10 mM sodium phosphate buffer (pH 7.0). <sup>b</sup>See Figure 1 for structures. <sup>c</sup>On the basis of first derivative analysis of changes in extinction coefficient at 260 nm for CT-DNA and 275 nm for poly d(AT) in the absence of compounds. <sup>d</sup>Binding constants based upon induced circular dichroism experiments (Figure 3). <sup>e</sup>Below the limit of detection (<10<sup>4</sup> M<sup>-1</sup>).

in Table 2. In the absence of the minor groove binding compounds, CT-DNA shows a positive band at 278 nm and a negative band at 245.2 nm at a concentration of 148 μM (Supporting Information). Similarly, poly d(A-T) shows a positive band at 166 nm and a negative band at 246.9 nm at a concentration of 143 μM (Supporting Information). Titration of 10 μM netropsin with CT-DNA and poly d(A-T) shows an ICD spectrum at 320 nm and gives a binding constant (*K*<sub>b</sub>) of 1.95 × 10<sup>5</sup> M<sup>-1</sup> and 2.44 × 10<sup>5</sup> M<sup>-1</sup>, respectively (Table 1 and Figure 3A,C). Interaction of 10 μM dipeptides **5** and **6** with CT-DNA and poly d(A-T) in the concentration range of 1 nM to 1 mM did not give rise to any ICD signal (data not shown). Therefore, the binding of the 2-ring compounds to these DNA substrates is too weak to be experimentally determined by any of the methods attempted. Upon interaction with CT-DNA, tripeptides **10** and **11** at 10 μM showed a positive signal at 325 nm (Figure 3E–H). The signal saturated at 1 mM of CT-DNA giving a *K*<sub>b</sub> of 2.88 × 10<sup>4</sup> M<sup>-1</sup> and 3.16 × 10<sup>4</sup> M<sup>-1</sup>, respectively, for **10** and **11** (Figure 3E,G). For the interaction of the compounds **10** and **11** with poly d(A-T), the value for the binding constant was found to be 1.95 × 10<sup>4</sup> and 1.81 × 10<sup>4</sup> at 325 nm, respectively (Figure 3F,H).

To understand the higher binding affinity provided by the extra pyrrolecarboxamide unit in the tripeptides and the effect of not being positively charged, the ICD maxima for the interactions of distamycin (10 μM) with CT-DNA and poly d(A-T) (Figure 3B,D) were measured and compared to those of netropsin (Figure 3A,C) and the tripeptides **10** and **11**. The *K*<sub>b</sub> for distamycin was calculated to be 2.10 × 10<sup>5</sup> M<sup>-1</sup> and 5.13 × 10<sup>5</sup> M<sup>-1</sup> for CT-DNA and poly d(A-T). Therefore, introduction of a single electrostatic interaction on the distamycin tripeptide due to the C-terminal guanidinium group results in approximately a 10-fold increase in binding

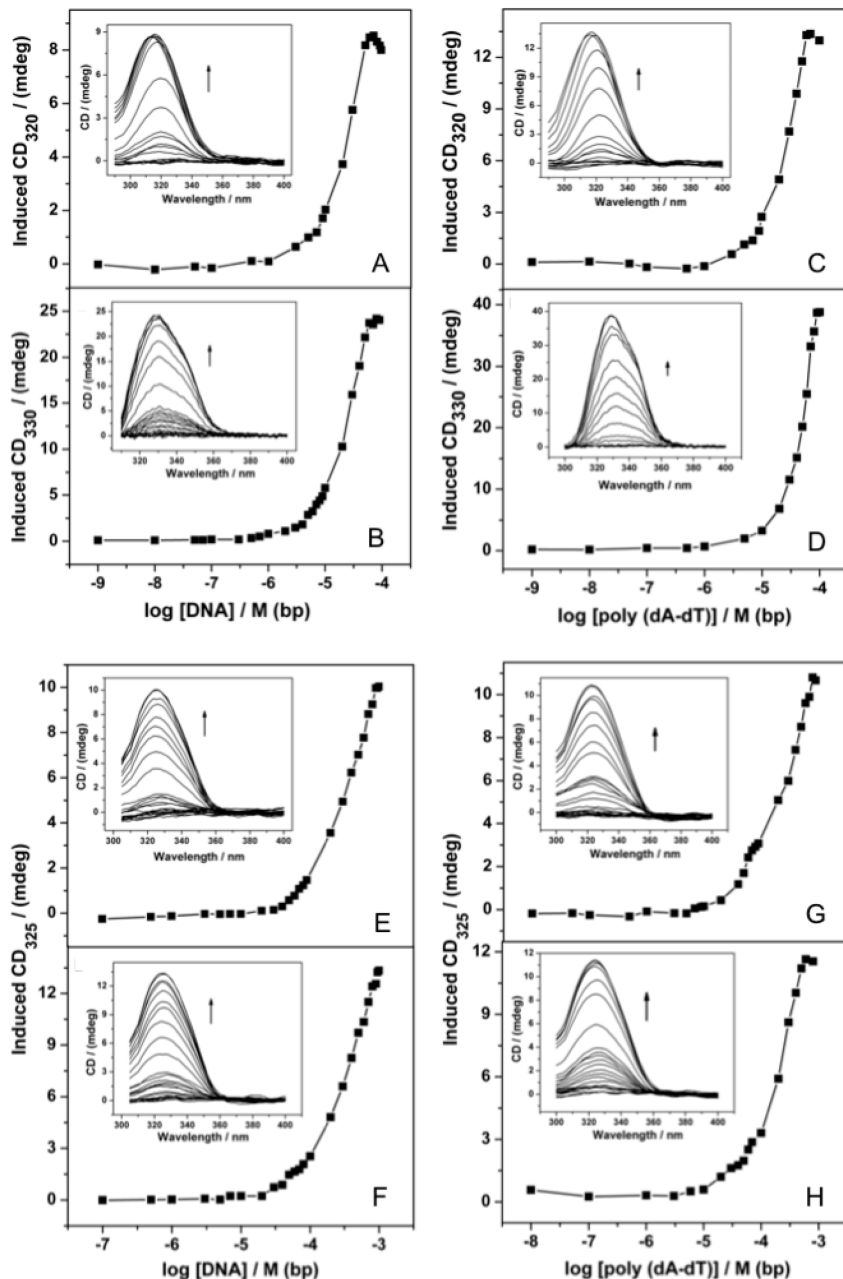


**Figure 3.** Titration curve of the ICD spectrum of sulfone derivatives of minor groove binders in 10% EtOH in phosphate buffer (pH 7) at 20 °C. CD of 10 μM minor groove binder in the presence of increasing concentrations (1 nM to 0.1 mM, base pairs) of CT DNA and poly d(A-T): inset the corresponding ICD spectra (the arrow indicates the increasing concentration of DNA): (A) netropsin + CT-DNA; (B) distamycin + CT-DNA; (C) netropsin + poly d(A-T); (D) distamycin + poly d(A-T); (E) **10** + CT-DNA; (F) **11** + CT-DNA; (G) **10** + poly d(A-T); (H) **11** + poly d(A-T). Binding constants were (Table 2) calculated using the nonlinear fit option in Origin software.

affinity versus neutral molecules **7** and **8**. The extra cationic amidinium group on the N-terminus of the netropsin dipeptide versus distamycin compensates for the one less pyrrolecarboxy amide subunit; both compounds have similar affinities for DNA.

**Toxicity in *E. coli*.** The toxicities of the di- and tripeptide methylating agents were evaluated in WT *E. coli* and in an *Alka/Tag* double mutant (Figure 4). The latter is defective in both of the known bacterial DNA-glycosylases that excise 3-mA. None of the compounds show any toxicity up to 10 μM concentration in WT bacteria. Presumably, efficient BER protects the WT cells from low levels of alkylation damage. In the glycosylase double mutant cell, the toxicity profiles of the

2-ring analogues are quite similar, which correlates with the in vitro formation of 3-mA for the different compounds (Figure 2A). For the tripeptide analogues, the toxicities followed the order of allyl (**8**) > propyl (**7**) > methoxyethyl (**9**). The tripeptides are between 2.5 and 3.0 orders of magnitude more toxic than the corresponding dipeptide compounds. This also correlates with the in vitro adduct data for **7** and **8** (Figure 2A).

**Toxicity in T98G Human Glioma Cells.** The toxicity of **1** and **7** was compared in WT T98G glioma cells using a short-term (72 h) MTS assay (Figure 5). Tripeptide **7** ( $LD_{50}$  19 μM) is >10-fold more toxic than dipeptide **1** ( $LD_{50}$  246 μM). Comparative toxicity experiments were performed with **1** in WT T98G cells and in cells engineered to overexpress (MPG+) (Figure 5).

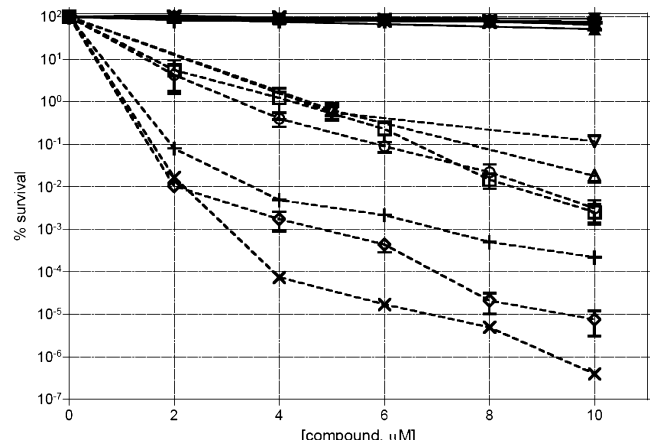


**Figure 4.** Toxicity of **1–4**, **7**, and **8** in wild type AB1157 *E. coli* (closed/bold symbols) and GC4803 *alkA/tag* glycosylase mutant cells (open symbols/lightface symbols): dipeptides **1** (■, □), **2** (●, ○), **3** (▲, Δ), and **4** (▼, ▽), and tripeptides **7** (◆, ◇), **8** (×, ×), and **9** (+, +). Midlog phase cells were exposed to varying concentrations of the analogues for 1 h, serially diluted, and their survival measured on solid LB media.

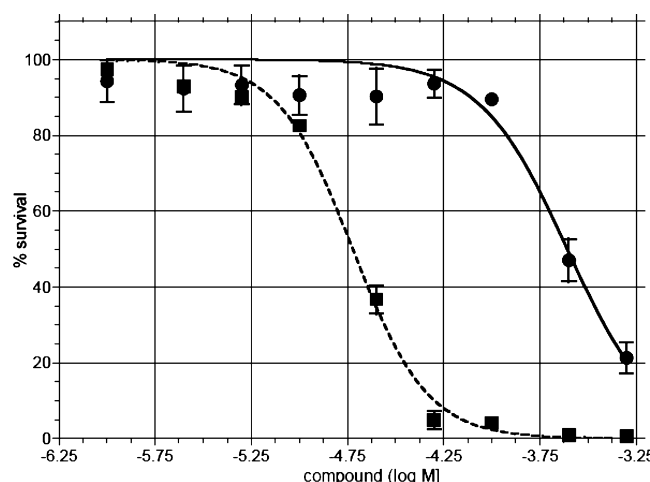


**Figure 5.** Toxicity in WT T98G cells exposed to varying concentrations of dipeptide **1** (●) and tripeptide **7** (■) after which cell survival was measured by a standard MTS assay. Data were fit using a nonlinear (curve-fit) in Prism software.

or under-express (MPG-) the human MPG glycosylase that mediates the excision of 3-mA in BER (Figure 6). In the overexpressing cells, there was a 10-fold increase in MPG mRNA and a very significant increase in protein expression.<sup>28</sup> In the MPG knockdown T98G cells, the expression for MPG is <5% of that in the WT cells.<sup>32</sup> There was no significant difference in the toxicity of **1** in the WT and MPG+ cells ( $LD_{50} \sim 240 \mu\text{M}$ ). However, the MPG- cells were 60% more sensitive relative to WT or MPG+ cells ( $LD_{50} 140$ ). The differences in toxicity parallel the activation of PARP and the formation of ARS (see below).

**Formation of Aldehyde Reactive Sites (ARS).** The apparent combined rates of formation and elimination of abasic sites and 5'-p-dR strand breaks were monitored in WT, MPG+, and MPG- T98G cells treated with equitoxic concentrations of **1** (80 μM) and **7** (7 μM). These concentrations were based upon their toxicity in the short term assay in WT cells (Figure 5). An aldehyde reactive hydrazine probe<sup>37–39</sup> that is biotin

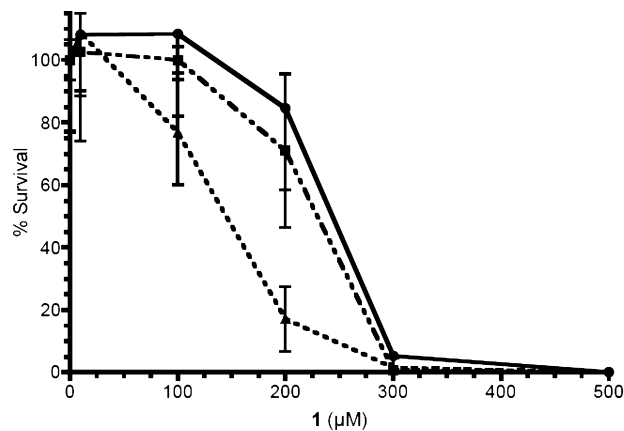


**Figure 6.** Toxicity of **1** in T98G glioma cells: wild type (WT, ●) and MPG overexpressing cells (MPG+, ■), and MPG knock down cells (MPG-, ▲). The cells were exposed to increasing concentrations of **1**, and survival was determined by the CyQuant assay 9 days after exposure, as described in the Experimental Procedures section.

conjugated with horseradish peroxidase (HRP) conjugated streptavidin (Figure 7) was used to label the ring-opened

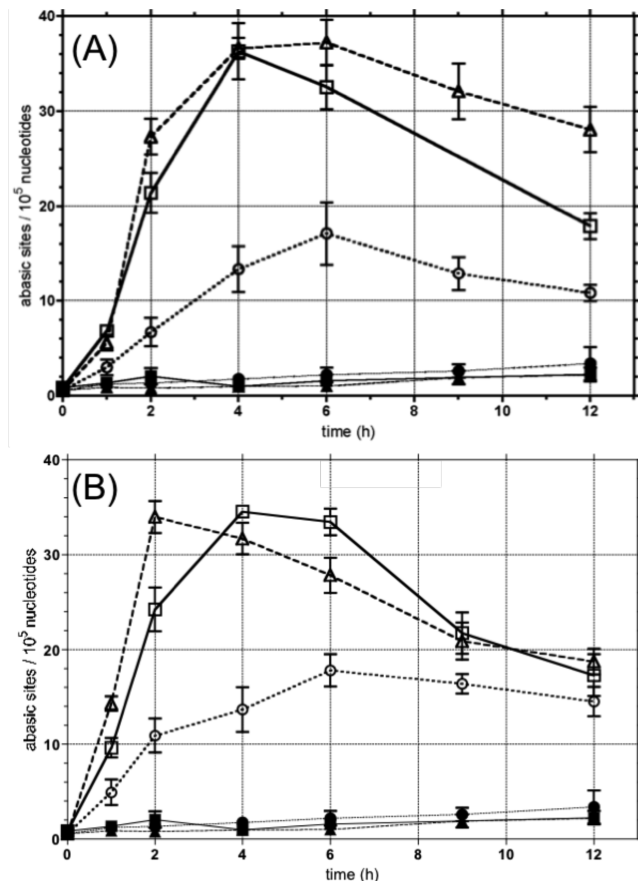


**Figure 7.** Time-dependent effect of di- and tripeptide methylating agents **1** and **7**, respectively, on the formation of aldehyde reactive sites (ARS) in WT, MPG overexpressing (MPG+), and MPG deficient (MPG-) T98G cells: (A) WT with DMSO (■), MPG+ with DMSO (▲), MPG- with DMSO (●), WT with 80 μM **1** (□), MPG+ with 80 μM **1** (Δ), MPG- with 80 μM **1** (○); (B) WT with DMSO (■), MPG+ with DMSO (▲), MPG- with DMSO (●), WT with 7 μM **7** (□), MPG+ with 7 μM **7** (Δ), and MPG- with 7 μM **7** (○).

aldehyde form of abasic sites, as well as other aldehyde groups that may be present. The level of aldehyde reactive sites (ARS) should correlate with the formation of the ring-opened form of the 1'-hydroxy-2'-deoxyribose group in abasic sites and 5'-p-dR termini.<sup>40</sup> Within the limits of detection, the background levels with just 0.5% DMSO are the same in all three cell lines. The initial rate of formation (up to 6 h) of ARS from **1** and **7** in WT cells is similar to that in MPG+ cells indicating that glycosylase excision of 3-mA is not limiting in WT cells. Moreover, the total ARS sustained for the time period monitored is virtually the same for both dipeptide **1** and tripeptide **7** at equitoxic concentrations. As anticipated, the MPG- cells respond differently: the rate of formation of ARS is slower, and the sustained level of ARS over the 12 h time course never reaches 50% of that observed in the WT and MPG+ cells.

As mentioned above, compounds **1** and **7** were compared to each other in WT, MPG+, and MPG- T98G cells using equitoxic concentrations in the WT cells. Because the number of WT cells in the cytotoxicity assay was  $1 \times 10^4$  cells/mL, whereas the ARS assay was done at a concentration of  $25 \times 10^4$  cells/mL, the toxicity in the latter will be significantly lower due to dilution of the methylating agent in 25-fold more cells. In addition, markers for apoptosis, e.g., caspase-3 and -7, appear elevated only after 12 h and only with the 250  $\mu\text{M}$  concentration, which is the LD<sub>50</sub> in the toxicity assay (Figure 5). Therefore, it is unlikely that a significant percentage of ARS is being measured in dead cells.

**PARP Activation and Cleavage.** PARP rapidly binds to single-strand breaks, such as the 5'-p-dR termini produced during BER, and synthesizes poly(ADP-ribose) chains.<sup>41-43</sup> The time course of PARP activation in the repair of 3-mA reflects the stage in BER in which APE-1 produces a strand break 5' of the abasic site created by MPG, which has no lyase activity. Therefore, the time course for PARP activation should be somewhat delayed relative to ARS formation. Little activation of PARP was observed after treating WT T98G cells with 80  $\mu\text{M}$  **1** (Figure 8A). This concentration corresponds to the LD<sub>10</sub> in the short term toxicity assay (Figure 5A). At 250  $\mu\text{M}$ , which corresponds to the LD<sub>50</sub> concentration, PARP activation reached a maximum level at 12 h and remained elevated up to 18 h (Figure 8A).

PARP activation by **1** was compared in the three cell lines. In WT and MPG+ cells treated with **1**, there was a dose-dependent increase in PAR deposition versus untreated cells. However, little change was observed in the MPG- knocked down cells treated with **1** (Figure 9). These data are consistent with the anticipated reduced rate of 3-mA lesions being converted into AP sites by MPG (Figure 7) and the subsequent APE1 mediated formation of 5'-dRP termini, which are substrates for PARP.

Caspase-3 and -7 activation, which is associated with apoptosis, results in the inactivation of PARP.<sup>44-46</sup> Therefore, caspase activity was monitored in the WT cells after treatment with 80 and 250  $\mu\text{M}$  **1** (Figure 8B). Caspase activation, which starts to climb by 12 h and continued to rise through 18 h, was only observed at the 250  $\mu\text{M}$  concentration of **1** indicating that the 80  $\mu\text{M}$  concentration is not toxic under the assay conditions. As predicted, cleavage of PARP was only significant with the concentration of **1** that induces caspase activation (Figure 8C). Little effect was seen at the lower concentration of **1**.

**Replication Tract Analysis.** There is in vitro evidence that 3-mA, as well as subsequent BER intermediates, can block

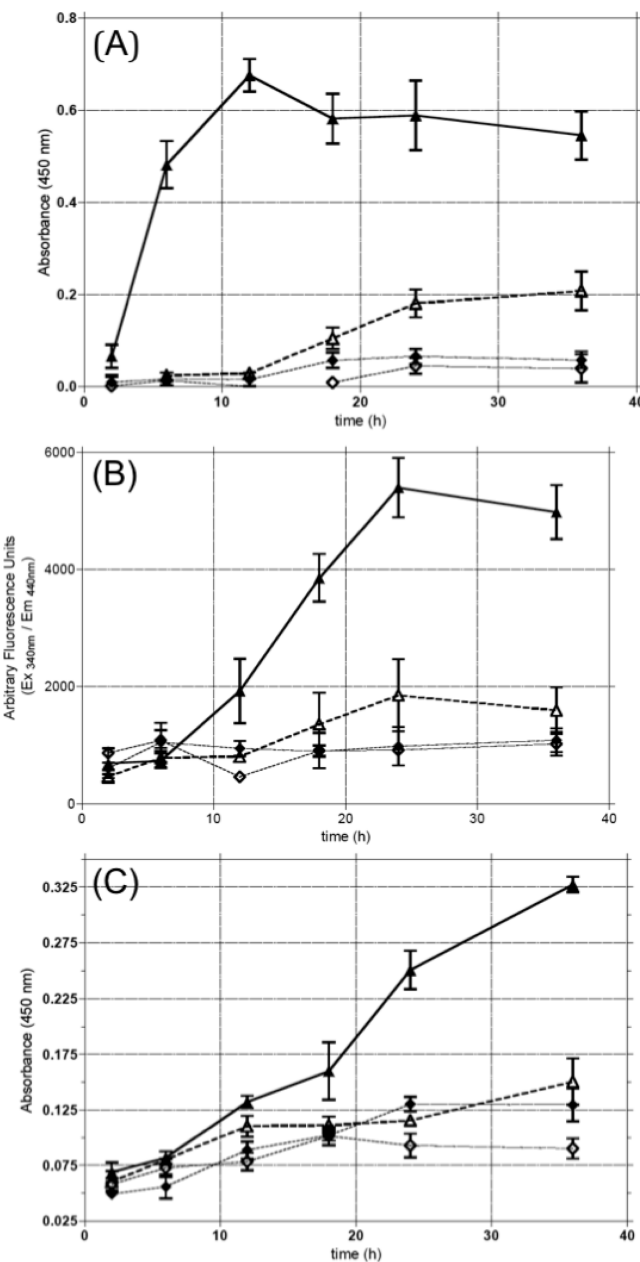
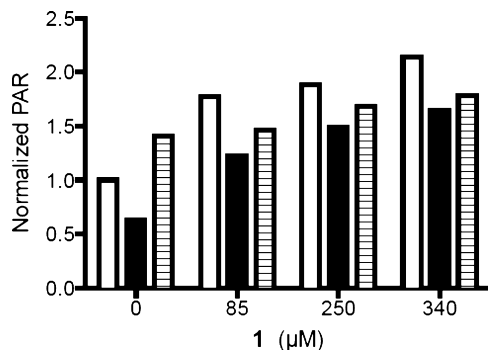


Figure 8. Time course for (A) PARP activation; (B) caspase-3 and -7 activation; and (C) cleavage of PARP in T98G WT cells, (◊) untreated; (◆) 0.2% DMSO; (Δ) 80  $\mu\text{M}$  **1**; (▲) 250  $\mu\text{M}$  **1**.

DNA replication.<sup>23-26</sup> To verify that this is the case in cells, a microfluidic assisted replication tract analysis<sup>36</sup> was performed in SF767 glioma cells treated with either 5 or 10  $\mu\text{M}$  of **1**. This assay uses antibodies to measure the length of replication tracts before the exposure of cells to alkylating agent **1** by monitoring 5-iodo-dU incorporation and after exposure to **1** by monitoring 5-chloro-dU incorporation. If the agent blocks replication, the length of the DNA stained with the 5-chloro-dU antibody will be shortened. The 40 min exposure of the glioma cells to 5  $\mu\text{M}$  **1** reduces clonogenic survival by 35%. The results appear in Figure 10 and show that track length at the 50 percentile was reduced from 7  $\mu\text{m}$  for untreated control cells to 5.7 and 4.0 for the 5 and 10  $\mu\text{M}$  concentrations of **1** (statistical difference with  $p \leq 0.001$ ). The data provide evidence that the formation of 3-



**Figure 9.** Normalized PAR production in T98G glioma cells: wild type (WT, filled columns) and MPG overexpressing cells (MPG+, open columns), and MPG knockdown cells (MPG-, hatched) as a function of the concentration of **1**.

679 mA directly or indirectly through BER intermediates impedes  
680 replication fork progression.

## 681 ■ DISCUSSION

**682 Relationship between DNA Methylation and DNA**  
**683 Binding.** Methylating agent **1** was developed as a strategy to  
684 selectively and efficiently generate 3-mA lesions both in vitro  
685 and in vivo.<sup>13–18</sup> The approach works quite well, but we have  
686 sought to improve on the design. Of note is the very weak  
687 equilibrium binding for the initially synthesized 2-ring  
688 compound. Despite this weak binding,<sup>18</sup> the alkylation pattern  
689 for **1** is very different from nonequilibrium binding methylating  
690 agents, e.g., methyl methanesulfonate (MMS), that predom-  
691 inantly yield the major groove adduct N7-methylguanine (7-  
692 mG).<sup>47</sup> The in vitro ratio for 3-mA (minor groove) to 7-mG  
693 (major groove) is approximately 3-orders of magnitude higher  
694 for **1** or **7** versus MMS. The methylation of DNA by **1** is clearly  
695 driven by the dipeptide binding in the minor groove to A/T  
696 rich regions and delivering the methyl group from the sulfonate  
697 ester.<sup>13,16–19</sup> In the current study, efforts to enhance  
698 methylating activity by changing the C-terminal group to  
699 improve water solubility and/or DNA binding were not  
700 successful. The major improvement came from adding another  
701 N-methylpyrrolecarboxamide subunit. In summary, the dipep-  
702 tides have binding affinities above 1 mM. The extra pyrrole  
703 subunit in the tripeptides, which provides an additional H-bond  
704 and a VDW contact, and displaces additional minor groove  
705 waters, increases the binding by more than 10-fold. It is of  
706 interest that despite the higher binding affinity of the

707 tripeptides for DNA and the higher levels of 3-mA that they  
708 produce (Figure 2A), the ratio of minor to major groove  
709 methylation does not radically differ (Figure 2B). The lack of a  
710 strong correlation between the specificity for minor groove  
711 methylation and minor groove binding affinity would suggest  
712 that the dipeptides preferentially populate the minor groove at  
713 A/T sequences but do not make the well-organized enthalpic  
714 interactions (H-bonds, VDW contacts) required for detection  
715 by ICD, isothermal titration calorimetry (ITC), or  $T_M$   
716 experiments.

**Mechanism of Action.** While the toxicity of the alkylating  
717 compounds used in the present study is highly associated with  
718 the yield of 3-mA, it remains unclear whether this lesion is  
719 directly responsible for the biological effects seen in cells. To  
720 further explore the mechanism(s) responsible for the toxicity,  
721 the compounds were evaluated in WT and *alkA/tag* glycosylase  
722 null *E. coli* cells. As expected, the WT cells were insensitive  
723 relative to the *alkA/tag* mutant due to efficient BER in the  
724 former.<sup>18</sup> This implies that the failure to initiate BER leads to  
725 persistent toxic 3-mA adducts. We have previously reported  
726 that the *alkA/tag* mutant is more sensitive to dipeptide **1** than  
727 cells defective in AP endonuclease activity (*apn* null cells)  
728 suggesting that 3-mA is more deleterious than an abasic site or  
729 other downstream BER intermediates.<sup>17,18</sup> The toxicity of **1** has  
730 been explored in WT *S. cerevisiae* and in a Mag1 glycosylase  
731 mutant (*mag1*), an AP endonuclease double mutant  
732 (*apn1apn2*), and a BER triple mutant (*mag1apn1apn2*).<sup>20</sup>  
733 The *apn1apn2* mutant was somewhat more sensitive to the  
734 toxicity of **1** than the *mag1* cells, while the triple mutant was  
735 even more sensitive. A *mag1rad14* double mutant yeast turned  
736 out surprisingly to be as sensitive to **1** as the *mag1apn1apn2*  
737 triple mutant, while the *rad14* single mutant showed no  
738 phenotype. This suggests an important role for nucleotide  
739 excision repair at some point in the processing of 3-mA but  
740 only if the initial glycosylase step in BER is blocked (Figure  
741 f11).  
742 f11

The story in the human cells is similar to that in *E. coli* and  
743 yeast. The T98G MPG- glioma cells, in which the human  
744 MPG protein that excises 3-mA is knocked down by 95%,<sup>32</sup> are  
745 about 60% more sensitive to the toxicity of **1** versus WT and  
746 MPG+ cells. This inverse correlation between the expression of  
747 the enzyme that removes 3-mA and the toxicity of **1** is  
748 consistent with the ARS data. The MPG- cells have  
749 significantly lower rates of formation and sustained levels of  
750 ARS than in the WT cells. Since the yield of 3-mA adducts  
751 produced by **1** and **7** should not be dependent on MPG levels,  
752 it is assumed that there will be more unrepaired 3-mA lesions in  
753

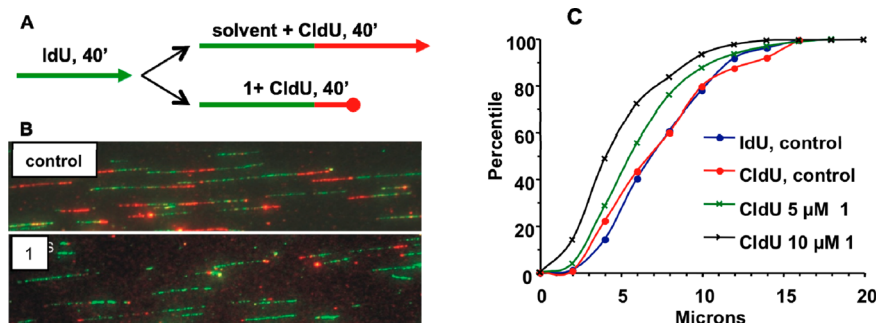


**Figure 10.** Microfluidic assisted replication tract analysis (ma-RTA) of A172 glioma cells without and with 40 min exposure to 5 and 10  $\mu\text{M}$  **1**: (A) experimental design; (B) images of micro track capillaries; (C) percentile analysis of track length ( $\mu\text{m}$ ) from B. The Kolmogorov–Smirnov (K-S) test was performed to determine the *P*-values of different cumulative distributions.

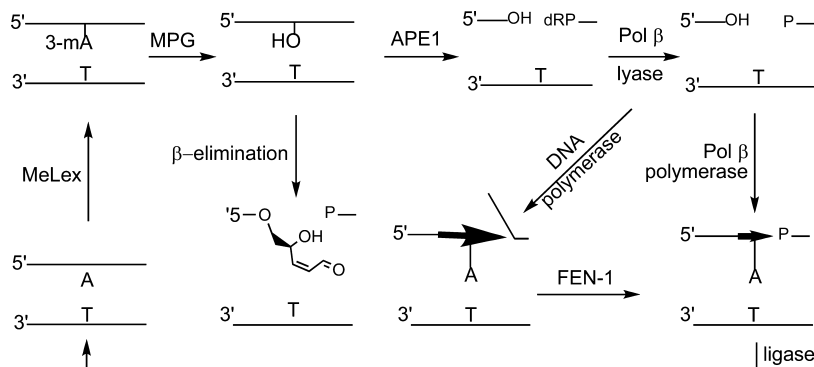


**Figure 11.** Repair of N3-methyladenine (3-mA) by base excision repair.

754 the MPG<sup>−</sup> cells. This would account for the lower ARS levels  
755 observed in these cells.

756 The fate of the unrepaired 3-mA adducts in the MPG<sup>−</sup> cells  
757 is unknown; however, the enhanced toxicity of **1** in the MPG  
758 knockdown cells indicates that 3-mA is either being converted  
759 by some process into a lethal intermediate or 3-mA directly  
760 blocks polymerases at replication forks. 3-mA can sponta-  
761 neously depurinate, especially in single-stranded DNA, to yield  
762 an AP site. If this were the case, APE1 cleavage at the AP site  
763 would cause PARP activation similar to that of the WT. This is  
764 not observed. We know **1** causes replication blocks in glioma  
765 cells exposed to low concentrations of **1** from the microfluidic  
766 assisted replication tract analysis of cells treated with **1** for 40  
767 min (Figure 10). Whether this is a direct effect or indirect effect  
768 of 3-mA remains to be determined, but it has been previously  
769 demonstrated that 3-mA and a stable analogue, 3-methyl-3-  
770 deazaadenine, directly block DNA polymerization in vitro.<sup>24–26</sup>

771 A significant sensitizing effect for the DNA methylating  
772 agents methyl methanesulfonate (MMS) (4-fold increase) and  
773 Temozolomide (10-fold increase) has been reported in human  
774 mammary gland cells that overexpress MPG.<sup>48</sup> Overexpression  
775 of a catalytically defective MPG mutant did not sensitize cells to  
776 either MMS or Temozolomide indicating the involvement of  
777 glycosylase activity. In contrast, the toxicity of **1** in the same  
778 MPG overexpressing cells was not enhanced versus WT cells.<sup>48</sup>  
779 As expected, the overexpression of MPG caused a significant  
780 increase in the rate of repair of 7-mG (3-mA levels were not  
781 followed) after MMS treatment. The authors suggested that the  
782 increase in toxicity was due to MPG mediated conversion of  
783 innocuous 7-mG lesions into toxic BER intermediates, e.g.,  
784 abasic sites. Other cell lines overexpressing MPG are also  
785 sensitive to MMS.<sup>49</sup> A similar modulation of MMS toxicity and  
786 mutagenicity was reported in CHO cells that overexpress the  
787 rat MPG protein.<sup>50</sup> To understand why the cellular level of  
788 MPG does not affect the toxicity of **1** and MMS in the same  
789 way, it is important to note that at equitoxic concentrations of  
790 MMS and **1** (based on their toxicity in WT cells), the yield of  
791 7-mG adducts will be substantially higher with MMS than with  
792 **1**. This is because of the difference in the ratio of 7-mG  
793 (nontoxic) to 3-mA (toxic): approximately 10:1 for MMS<sup>47</sup>  
794 and 1:100 for **1**. The conversion of nontoxic 7-mG to toxic  
795 intermediates by BER nicely explains the differential impact of  
796 MPG overexpression on MMS versus **1**.<sup>48</sup>

797 The level of ARS is also a function of APE-1 endonuclease  
798 activity that converts abasic sites into 5'-p-dR lesions, which  
799 retain the reactive aldehyde functionality (Figure 11). Because  
800 the number of APE-1 molecules in cells is estimated to be  
801 between 4 and  $70 \times 10^5$  per cell,<sup>51</sup> Pol  $\beta$ , and not APE-1 or

MPG, is normally considered the rate limiting step in BER.<sup>52</sup> However, antisense suppression of MPG or APE-1 enhances the toxicity of **1** suggesting that unrepaired 3-mA is cytotoxic.<sup>53</sup> We have also shown using a small molecule inhibitor of APE-1 that the level and persistence of ARS in WT T98G cells continues to increase through 12 h after treatment with **1**,<sup>54</sup> while the level falls off after 6 h in cells treated with **1** alone (Figure 7). The inhibition of APE-1 endonuclease activity synergistically enhanced the toxicity of **1** in T98G cells consistent with the toxicity of unrepaired abasic sites. Clearly, both unrepaired 3-mA, abasic sites, or other BER intermediates are cytotoxic.

In summary, a number of minor groove alkylating compounds were prepared and evaluated based on their ability to bind to and methylate DNA. As expected, there is a direct relationship between DNA binding, formation of 3-mA, and toxicity. Moreover, the rate and extent of excision of 3-mA by human MPG and the formation of ARS inversely correlate with toxicity. These data indicate that 3-mA can directly cause toxicity, most likely due to its ability to block DNA replication, and that there is no need for it to be converted into a downstream BER intermediate.

## ASSOCIATED CONTENT

### Supporting Information

Synthetic details, NMR, MS spectra, HPLC traces, and stability study details. This material is available free of charge via the Internet at <http://pubs.acs.org>.

## AUTHOR INFORMATION

### Corresponding Author

\*Tel: 1-412-383-9593. E-mail: goldbi@pitt.edu.

### Funding

This work was supported in part by National Institutes of Health grants CA29088 (to B.G.), CA148629 (to R.W.S.), and GM087798 (to R.W.S.). Support for the UPCI Lentiviral Facility was provided by the Cancer Center Support Grant CA047904 from the National Institutes of Health.

### Notes

The authors declare the following competing financial interest(s): R.W.S. is a scientific consultant for Trevigen, Inc.

## ACKNOWLEDGMENTS

We gratefully acknowledge Julia Sidorova (Department of Pathology, University of Washington) for her support and guidance on the microfluidic assisted replication tract analysis assay.

## 846 ■ ABBREVIATIONS

847 AlkA, *E. coli* 3-methyladenine-DNA glycosylase II; ARS,  
 848 aldehyde reactive site; BER, base excision repair; CD, circular  
 849 dichroism; ICD, induced circular dichroism; ITC, isothermal  
 850 titration calorimetry; 3-mA, N3-methyladenine; 7-mG, N7-  
 851 methylguanine; MPG, (aka, AAG) methylpurine-DNA glyco-  
 852 sylase; MPG+, MPG overexpressing T98G cells; MPG-, MPG  
 853 knockdown T98G cells; PARP, poly(ADP-ribose)polymerase;  
 854 TAG, *E. coli* 3-methyladenine DNA glycosylase I; WT, wild  
 855 type

## 856 ■ REFERENCES

- 857 (1) Pratt, W. B., Rudden, R. W., Ensminger, W. D., and Maybaum, J.,  
 858 Eds. (1994) *The Anticancer Drugs*, 2nd ed., Oxford Press, New York.  
 859 (2) See <http://monographs.iarc.fr/ENG/Classification/>.
- 860 (3) Shrivastav, N., Li, D., and Essigmann, J. M. (2010) Chemical  
 861 biology of mutagenesis and DNA repair: cellular responses to DNA  
 862 alkylation. *Carcinogenesis* 31, 59–70.
- 863 (4) Marchesi, F., Turziani, M., Tortorelli, G., Avvisati, G., Torino,  
 864 F., and De Vecchis, L. (2007) Triazene compounds: mechanism of  
 865 action and related DNA repair systems. *Pharmacol. Res.* 56, 275–287.
- 866 (5) Hijiya, N., Hudson, M. M., Lensing, S., Zacher, M., Onciu, M.,  
 867 Behm, F. G., Razzouk, B. I., Ribeiro, R. C., Rubnitz, J. E., Sandlund, J. T.,  
 868 Rivera, G. K., Evans, W. E., Relling, M. V., and Pui, C. H. (2007)  
 869 Cumulative incidence of secondary neoplasms as a first event after  
 870 childhood acute lymphoblastic leukemia. *J. Am. Med. Assoc.* 297,  
 871 1207–1215.
- 872 (6) Hijiya, N., Ness, K. K., Ribeiro, R. C., and Hudson, M. M. (2009)  
 873 Acute leukemia as a secondary malignancy in children and adolescents:  
 874 current findings and issues. *Cancer* 115, 23–35.
- 875 (7) Türk, D., and Szakács, G. (2009) Relevance of multidrug  
 876 resistance in the age of targeted therapy. *Curr. Opin. Drug Discovery*  
 877 Dev. 12, 246–252.
- 878 (8) Baumert, C., and Hilgeroth, A. (2009) Recent advances in the  
 879 development of P-gp inhibitors. *Anticancer Agents Med. Chem.* 9, 415–  
 880 436.
- 881 (9) Gangemi, R., Paleari, L., Orengo, A. M., Cesario, A., Chessa, L.,  
 882 Ferrini, S., and Russo, P. (2009) Cancer stem cells: a new paradigm for  
 883 understanding tumor growth and progression and drug resistance.  
 884 *Curr. Med. Chem.* 16, 1688–1703.
- 885 (10) Baguley, B. C. (2010) Multiple drug resistance mechanisms in  
 886 cancer. *Mol. Biotechnol.* 46, 308–316.
- 887 (11) Liu, J., Powell, K. L., Thame, H. D., and MacLeod, M. C.  
 888 (2010) Detoxification of sulfur half-mustards by nucleophilic  
 889 scavengers: robust activity of thiopurines. *Chem. Res. Toxicol.* 23,  
 890 488–496.
- 891 (12) Abel, E. L., Bubel, J. D., Simper, M. S., Powell, L., McClellan, S. A., Andreeff, M., MacLeod, M. C., and DiGiovanni, J. (2010)  
 893 Protection against 2-chloroethyl ethyl sulfide (CEES)-induced  
 894 cytotoxicity in human keratinocytes by an inducer of the glutathione  
 895 detoxification pathway. *Toxicol. Appl. Pharmacol.* 255, 176–183.
- 896 (13) Zhang, Y., Chen, F.-X., Mehta, P., and Gold, B. (1993) The  
 897 design of groove and sequence selective alkylation of DNA by  
 898 sulfonate esters tethered to lexitropsins. *Biochemistry* 32, 7954–7965.
- 899 (14) Encell, L., Shuker, D. E. G., Foiles, P. G., and Gold, B. (1996)  
 900 The in vitro methylation of DNA by a minor groove binding methyl  
 901 sulfonate ester. *Chem. Res. Toxicol.* 9, 563–567.
- 902 (15) Kelly, J., Shah, D., Chen, F.-X., Wurdean, R., and Gold, B.  
 903 (1998) Quantitative and qualitative analysis of DNA methylation at  
 904 N3-adenine by N-methyl-N-nitrosourea and dimethyl sulfate. *Chem.*  
 905 *Res. Toxicol.* 11, 1481–1486.
- 906 (16) Varadarajan, S., Shah, D., Dande, P., Settles, S., Chen, F.-X.,  
 907 Fronza, G., and Gold, B. (2003) DNA damage and cytotoxicity  
 908 induced by minor groove binding methyl sulfonate esters. *Biochemistry*  
 909 42, 14318–14327.
- 910 (17) Shah, D., and Gold, B. (2003) Evidence in *Escherichia coli* that  
 911 N3-methyladenine lesions and cytotoxicity induced by a minor groove  
 binding methyl sulfonate ester can be modulated in vivo by netropsin. 912  
*Biochemistry* 42, 12610–12616. 913
- (18) Shah, S., Kelly, J., Zhang, Y., Dande, P., Martinez, J., Ortiz, G., 914  
 Fronza, G., Tran, H., Soto, M. A., Marky, L., and Gold, B. (2001) 915  
 Evidence in *Escherichia coli* that N3-methyladenine lesions induced by 916  
 a minor groove binding methyl sulfonate ester can be processed by 917  
 both base and nucleotide excision repair. *Biochemistry* 40, 1796–1803. 918
- (19) Kelly, J., Inga, A., Chen, F.-X., Dande, P., Shah, D., Monti, P., 919  
 Aprile, A., Burns, P. A., Scott, G., Abbondandolo, A., Gold, B., and 920  
 Fronza, G. (1999) Relationship between DNA methylation and 921  
 mutational patterns induced by a sequence selective minor groove 922  
 methylating agents. *J. Biol. Chem.* 274, 18327–18334. 923
- (20) Monti, P., Campomenosi, P., Iannone, R., Ciribilli, Y., Iggo, 924  
 R., Scott, G., Burns, P. A., Shah, D., Menichini, P., Abbondandolo, A., 925  
 Gold, B., and Fronza, G. (2002) Influences of base excision repair 926  
 defects on the lethality and mutagenesis induced by Me-lex, a sequence 927  
 selective N3-adenine methylating agent. *J. Biol. Chem.* 277, 28663– 928  
 28668. 929
- (21) Monti, P., Iannone, R., Campomenosi, P., Ciribilli, Y., Robbiano, 930  
 A., Varadarajan, S., Shah, D., Menichini, P., Gold, B., and Fronza, G. 931  
 (2004) Nucleotide excision repair defect influences lethality and 932  
 mutagenicity induced by Me-lex, a sequence-selective N3-adenine 933  
 methylating agent in the absence of base excision repair. *Biochemistry* 934  
 43, 5592–2299. 935
- (22) Monti, P., Ciribilli, Y., Russo, D., Bisio, A., Perfumo, C., 936  
 Andreotti, V., Menichini, P., Inga, A., Huang, X., Gold, B., and Fronza, 937  
 G. (2008) REV1 and Pol $\zeta$  influence toxicity and mutagenicity of Me- 938  
 lex, a sequence selective N3-adenine methylating agent. *DNA Repair* 7, 939  
 431–438. 940
- (23) Boiteux, S., Huisman, O., and Laval, J. (1984) 3-Methyladenine 941  
 residues in DNA induce the SOS function *sfiA* in *Escherichia coli*. 942  
*EMBO J.* 3, 2569–2573. 943
- (24) Larson, K., Sahm, J., Shenkar, R., and Strauss, B. (1985) 944  
 Methylation-induced blocks to in vitro DNA replication. *Mutat. Res.* 945  
 150, 77–84. 946
- (25) Plosky, B. S., Frank, E. G., Berry, D. A., Vennall, G. P., 947  
 McDonald, J. P., and Woodgate, R. (2008) Eukaryotic Y-family 948  
 polymerases bypass a 3-methyl-2'-deoxyadenosine analog in vitro and 949  
 methyl methanesulfonate-induced DNA damage in vivo. *Nucleic Acids* 950  
*Res.* 36, 2152–2162. 951
- (26) Settles, Wang, R.-W., Fronza, G., and Gold, B. (2010) Effect of 952  
 N3-Methyladenine and an isosteric stable analogue on DNA 953  
 polymerization. *J. Nucleic Acids* 2010, 426505. 954
- (27) Monti, P., Broxson, C., Inga, A., Wang, R.-W., Menichini, P., 955  
 Tornaletti, S., Gold, B., and Fronza, G. (2011) 3-Methyl-3- 956  
 deazaadenine, a stable isostere of N3-methyl-adenine, is efficiently 957  
 bypassed by replication in vivo and by transcription in vitro. *DNA* 958  
*Repair* 10, 861–868. 959
- (28) Tang, J. B., Svilar, D., Trivedi, R. N., Wang, X. H., Goellner, E. 960  
 M., Moore, B., Hamilton, R. L., Banze, L. A., Brown, A. R., and Sobol, 961  
 R. W. (2011) N-methylpurine DNA glycosylase and DNA polymerase 962  
 beta modulate BER inhibitor potentiation of glioma cells to 963  
*Temozolomide*. *Neuro. Oncol.* 13, 471–486. 964
- (29) Tang, J., Goellner, E. M., Wang, X. W., Trivedi, R. N., St. Croix, 965  
 C. M., Jelezova, E., Svilar, D., Brown, A. R., and Sobol, R. W. (2010) 966  
 Bioenergetic metabolites regulate base excision repair-dependent cell 967  
 death in response to DNA damage. *Mol. Cancer Res.* 8, 67–79. 968
- (30) Mutamba, J. T., Svilar, D., Prasongtanakij, S., Wang, X. H., Lin, 969  
 Y. C., Dedon, P. C., Sobol, R. W., and Engelward, B. P. (2011) XRCC1 970  
 and base excision repair balance in response to nitric oxide. *DNA* 971  
*Repair* 10, 1282–1293. 972
- (31) Svilar, D., Vens, C., and Sobol, R. W. (2012) Quantitative, real- 973  
 time analysis of base excision repair activity in cell lysates utilizing 974  
 lesion-specific molecular beacons. *J. Vis. Exp.* 66, e4168. 975
- (32) Svilar, D., Dyavaiah, M., Brown, A. R., Tang, J. B., Li, J., 976  
 McDonald, P. R., Shun, T. Y., Braganza, A., Wang, X. H., Maniar, S., St 977  
 Croix, C. M., Lazo, J. S., Pollack, I. F., Begley, T. J., and Sobol, R. W. 978  
 (2012) Alkylation sensitivity screens reveal a conserved cross-species 979  
 functionome. *Mol. Cancer Res.*, published Online Nov 27, 2012. 980

- 981 (33) Baird, E. E., and Dervan, P. B. (1996) Solid phase synthesis of 982 polyamides containing imidazole and pyrrole amino acids. *J. Am. 983 Chem. Soc.* 118, 6141–6146.
- 984 (34) Wurtz, N. R., Turner, J. M., Baird, E. E., and Dervan, P. B. 985 (2001) Fmoc solid phase synthesis of polyamides containing pyrrole 986 and imidazole amino acids. *Org. Lett.* 3, 1201–1203.
- 987 (35) Garbett, N. C., Ragazzon, P. A., and Chaires, J. B. (2007) 988 Circular dichroism to determine binding mode and affinity of ligand- 989 DNA interactions. *Nat. Protoc.* 2, 3166–3172.
- 990 (36) Sidorova, J. M., Li, N., Schwartz, D. C., Folch, A., and Monnat, 991 R. J., Jr. (2009) Microfluidic-assisted analysis of replicating DNA 992 molecules. *Nat. Protoc.* 4, 849–861.
- 993 (37) Kubo, K., Ide, H., Wallace, S. S., and Kow, Y. W. (1992) A 994 novel, sensitive, and specific assay for abasic sites, the most commonly 995 produced DNA lesion. *Biochemistry* 31, 3703–3708.
- 996 (38) Kow, Y. W., and Dare, A. (2000) Detection of abasic sites and 997 oxidative DNA base damage using an ELISA-like assay. *Methods* 22, 998 164–169.
- 999 (39) Nakamura, J., Walker, V. E., Upton, P. B., Chiang, S. Y., Kow, Y. 1000 W., and Swenberg, J. A. (1998) Highly sensitive apurinic/apirimidinic 1001 site assay can detect spontaneous and chemically induced depurination 1002 under physiological conditions. *Cancer Res.* 58, 222–225.
- 1003 (40) Bennett, S. E., and Kitner, J. (2006) Characterization of the 1004 aldehyde reactive probe reaction with AP-sites in DNA: influence of 1005 AP-lyase on adduct stability. *Nucleosides, Nucleotides Nucleic Acids* 25, 1006 823–842.
- 1007 (41) Dantzer, F., Schreiber, V., Niedergang, C., Trucco, C., Flatter, 1008 E., De La Rubia, G., Oliver, J., Rolli, V., Ménissier-de Murcia, J., and de 1009 Murcia, G. (1999) Involvement of poly(ADP-ribose) polymerase in 1010 base excision repair. *Biochimie* 81, 69–75.
- 1011 (42) Khodyreva, S. N., Prasad, R., Ilina, E. S., Sukhanova, M. V., 1012 Kutuzov, M. M., Liu, Y., Hou, E. W., Wilson, S. H., and Lavrik, O. I. 1013 (2010) Apurinic/apirimidinic (AP) site recognition by the 5'-dRP/AP 1014 lyase in poly(ADP-ribose) polymerase-1 (PARP-1). *Proc. Natl. Acad. 1015 Sci. U.S.A.* 107, 22090–22095.
- 1016 (43) Eustermann, S., Videler, H., Yang, J. C., Cole, P. T., Gruszka, D., 1017 Veprintsev, D., and Neuhaus, D. (2011) The DNA-binding domain of 1018 human PARP-1 interacts with DNA single-strand breaks as a 1019 monomer through its second zinc finger. *J. Mol. Biol.* 407, 149–170.
- 1020 (44) Lazebnik, Y. A., Kaufmann, S. H., Desnoyers, S., Poirier, G. G., 1021 and Earnshaw, W. C. (1994) Cleavage of poly(ADP-ribose) 1022 polymerase by a proteinase with properties like ICE. *Nature* 371, 1023 346–347.
- 1024 (45) Nicholson, D. W., and Thornberry, N. A. (1997) Caspases: 1025 killer proteases. *Trends Biochem. Sci.* 22, 299–306.
- 1026 (46) Germain, M., Affar, E. B., D'Amours, D., Dixit, V. M., Salvesen, 1027 G. S., and Poirier, G. G. (1999) Cleavage of automodified poly(ADP- 1028 ribose) polymerase during apoptosis. Evidence for involvement of 1029 caspase-7. *J. Biol. Chem.* 274, 28379–28384.
- 1030 (47) Beranek, D. T., Weis, C. C., and Swenson, D. H. (1980) A 1031 comprehensive quantitative analysis of methylated and ethylated DNA 1032 using high pressure liquid chromatography. *Carcinogenesis* 1, 595–606.
- 1033 (48) Rinne, M. L., He, Y., Pachkowski, B. F., Nakamura, J., and 1034 Kelley, M. R. (2005) N-methylpurine DNA glycosylase overexpression 1035 increases alkylation sensitivity by rapidly removing non-toxic 7- 1036 methylguanine adducts. *Nucleic Acids Res.* 33, 2859–2867.
- 1037 (49) Goellner, E. M., Grimme, B., Brown, A. R., Lin, Y. C., Wang, X. 1038 H., Sugrue, K. F., Mitchell, L., Trivedi, R. N., Tang, J. B., and Sobol, R. 1039 W. (2011) Overcoming Temozolomide resistance in glioblastoma via 1040 dual inhibition of NAD<sup>+</sup> biosynthesis and base excision repair. *Cancer 1041 Res.* 71, 2308–2317.
- 1042 (50) Calléja, F., Jansen, J. G., Vrielink, H., Laval, F., and van Zeeland, 1043 A. A. (1999) Modulation of the toxic and mutagenic effects induced by 1044 methyl methanesulfonate in Chinese hamster ovary cells by over- 1045 expression of the rat N-alkylpurine DNA-glycosylase. *Mutat. Res.* 425, 1046 185–194.
- 1047 (51) Chen, D. S., Herman, T., and Demple, B. (1991) Two distinct 1048 human DNA diesterases that hydrolyze 3'-blocking deoxyribose 1049 fragments from oxidized DNA. *Nucleic Acids Res.* 19, 5907–5914.
- (52) Srivastava, D. K., Vande Berg, B. J., Prasad, R., Molina, J. T., Beard, W. A., Tomkinson, A. E., and Wilson, S. H. (1998) Mammalian abasic site base excision repair. Identification of the reaction sequence and rate-determining steps. *J. Biol. Chem.* 273, 21203–21209.
- (53) Bobola, M. S., Varadarajan, S., Smith, N. W., Goff, R. D., Kolstoe, D. D., Blank, A., Gold, B., and Silber, J. R. (2007) Human glioma cell sensitivity to the sequence-specific alkylating agent methyl-lexitropsin. *Clin. Cancer Res.* 13, 612–620.
- (54) Srinivasan, A., Wang, L., Cline, C. J., Xie, Z., Sobol, R. W., Xie, X.-Q., and Gold, B. (2012) The identification and characterization of human AP endonuclease-1 inhibitors. *Biochemistry* 51, 6246–6259.